PNAS
www.pnas.org

Main Manuscript for

Fossilized cell structures identify an ancient origin for the teleost whole-genome duplication.

Donald Davesne[1,2,3*], Matt Friedman[4], Armin D. Schmitt[1,5], Vincent Fernandez[6,7], Giorgio Carnevale[8], Per E. Ahlberg[9], Sophie Sanchez[6,9], Roger B. J. Benson[1,*]

[1]Department of Earth Sciences, University of Oxford, Oxford, UK

[2]Institut de Systématique, Évolution, Biodiversité, UMR 7205 (MNHN – Sorbonne Université – CNRS – EPHE), Muséum national d'Histoire naturelle, Paris, France

[3]Museum für Naturkunde, Leibniz-Institut für Evolutions- und Biodiversitätsforschung, Berlin, Germany

[4]Museum of Paleontology and Department of Earth and Environmental Sciences, University of Michigan, Ann Arbor, USA

[5]Department of Earth Sciences, University of Cambridge, Cambridge, UK

[6]European Synchrotron Radiation Facility, Grenoble, France

[7]Imaging and Analysis Centre, Natural History Museum, London, UK

[8]Dipartimento di Scienze della Terra, Università degli Studi di Torino, Turin, Italy

[9]Subdepartment of Evolution and Development, Department of Organismal Biology, Uppsala University, Uppsala, Sweden

*Corresponding authors: Donald Davesne and Roger B. J. Benson.

Email: donald.davesne@gmail.com; roger.benson@earth.ox.ac.uk

Author Contributions: D.D., M.F. P.E.A., S.S. and R.B.J.B. conceived and designed the project. D.D., M.F., G.C. and R.B.J.B. collected and prepared the material. D.D., A.D.S, V.F., S.S. and R.B.J.B. performed the synchrotron experiments. V.F. and S.S. prepared the PPC-SRμCT scan data and provided training for their reconstruction. A.D.S. segmented the scan data. D.D., A.D.S., S.S. and R.B.J.B. analysed the data. All authors discussed the interpretations. D.D., M.F. and

R.B.J.B. developed the main text and made the figures. D.D., V.F. and G.C. wrote the SI Appendix. All authors provided a critical review of the manuscript and approved the final draft.

Competing Interest Statement: The authors declare no conflict of interest.

Classification: Biological Sciences, Evolution

Keywords: Actinopterygii, Teleostei, whole-genome duplication, osteocytes, paleontology.

This PDF file includes:

Main Text
Figures 1 to 2

Abstract

Teleost fishes comprise half of all vertebrate species, and possess a duplicated genome. This whole-genome duplication (WGD) occurred on the teleost stem-lineage, in an ancient common ancestor of all living teleosts, and is hypothesized as a trigger of their exceptional evolutionary radiation. Genomic and phylogenetic data indicate that WGD occurred in the Mesozoic, after the divergence of teleosts from their closest living relatives, but before the origin of the extant teleost groups. However, these approaches cannot pinpoint WGD among the many extinct groups that populate this 50- to 100-million-year lineage, preventing tests of the evolutionary effects of WGD. We infer patterns of genome size evolution in fossil stem-group teleosts using high-resolution synchrotron X-ray tomography to measure the bone cell volumes, which correlate with genome size in living species. Our findings indicate that WGD occurred very early on the teleost stem-lineage, and that all extinct stem-group teleosts known so far possessed duplicated genomes. WGD therefore substantially pre-dates both the origin of proposed key innovations of the teleost skeleton and the onset of substantial morphological diversification in the clade. Moreover, the early occurrence of WGD allowed considerable time for post-duplication reorganization prior to the origin of the teleost crown-group. This suggests at most an indirect link between WGD and evolutionary success, with broad implications for the relationship between genomic architecture and large-scale evolutionary patterns in the vertebrate Tree of Life.

Significance Statement

Some lineages of organisms have undergone major evolutionary radiations, while others have not. Establishing why is a central goal of evolutionary research. Whole-genome duplication (WGD) is often proposed as having caused the spectacular evolutionary radiation of teleost fishes. However, due to the absence of genetic data for fossil species, it has been impossible to pinpoint precisely when WGD occurred during teleost history. We use 3D measurements of fossilized bone cell spaces to estimate genome sizes in extinct species, observing a near-doubling of size during earliest teleost ancestry. This suggests that WGD occurred very early, substantially pre-dating the dramatic radiation of teleosts. These findings suggest at most and indirect link between WGD and teleost diversification.

Main Text

Introduction

Whole-genome duplication (WGD) has occurred independently in multiple lineages of plants, fungi, and animals (1–3). This represents a major change to genomic architecture, with hypothesized impacts on evolutionary diversification (4, 5), caused by the origin of new gene functions from duplicate copies, expanding the genetic toolbox available for evolutionary 'tinkering' (6). However, in spite of its mechanistic plausibility, this hypothesis is so far supported by only limited and contradictory empirical evidence (7–10). Teleost fishes – comprising more than half of modern vertebrates – are a key example, with their spectacular variety of form and kind (ranging from eels to seahorses) often viewed as *prima facie* evidence for the role of WGD in triggering evolutionary diversification (6, 11). Teleost also show an incredible diversity of genome biology, demonstrating particularly high rates of evolution of protein-coding genes (12) and non-coding elements (13), a broad range of genome sizes including the smallest vertebrate genomes (14), and multiple polyploid lineages (15).

The genome of all living teleosts derives from an ancient WGD event that occurred before the last common ancestor of modern species (16). Additional duplication events occurred more recently in several teleost subgroups (9, 17), but are not generally proposed as drivers of diversification (9). Studies of the role of WGD in contributing to teleost diversity so far have analyzed the distribution of species richness among extant lineages and morphometric data for fossil phenotypes, with potentially conflicting results: extant teleosts have high rates of lineage diversification compared to other ray-finned fishes (7), but early fossil members of the teleost crown-group do not show increased rates of morphological evolution (18).

Molecular phylogenetic studies indicate that WGD occurred on the teleost stem-lineage: after the divergence of teleosts from their extant sister taxon (Holostei), but before the most recent common ancestor of all living teleosts (19, 20). However, these bounds encompass a large phylogenetic diversity of extinct groups that diverged during an interval of 50–100 million years, from the initial divergence of the teleost total-group from the holostean total-by the earliest Triassic (21), up to the first appearance of crown-group teleosts in the Late Jurassic (18, 22). Molecular-clock estimates provide only broad constraints on the precise timing of duplication (316-226 Ma (23); ~310 Ma (24)), and offer no information on its phylogenetic position on the teleost stem lineage. The imprecision of these estimates and the sometimes considerable incongruence of molecular clocks with the teleost fossil record questions the reliability of these inferences in the absence of further evidence.

Patterns of genome size evolution on the teleost stem lineage could provide alternative and independent evidence on the timing and phylogenetic position of the teleost WGD. However, stem lineages by definition comprise entirely extinct species that are known only from fossils, for which genomic data are absent. Nevertheless, some information about vertebrate genome size is preserved within fossil bone (25–27). Living organisms show a positive correlation between cell size and genome size (28–30), such that the volumes of bone cell spaces (osteocyte lacunae) allow estimates of genome size. This relationship has been demonstrated in ray-finned fishes, including teleosts, and is predictive for large-scale variation in genome size (31). The precision of this approach is sufficient for inferring the large change (presumably, doubling) of genome size involved in WGD (31). Here, we use this relationship to trace the evolution of genome size in extinct ray-finned fishes, using osteocyte lacuna volumes as a proxy for genome size. Our sample includes a broad range of stem- and crown-group teleosts, providing information on patterns of teleost genome-size evolution during the deep evolutionary history of the teleost total-group.

Three-dimensional measurement of fossil bone cell spaces with µm-scale diameters presents considerable technical challenges. We used propagation phase contrast synchrotron radiation X-ray micro-computed tomography (PPC-SRµCT) to address this, collecting standardized measurements of osteocyte lacuna volumes for 61 fossil ray-finned fish species ranging from 2.5 to 252 million years in age (*SI Appendix, Part I*). This fossil evidence is complemented by data from a previous study including 34 modern ray-finned fish species with known genome sizes (31). Our fossil sample includes all major groups of stem-group teleosts, members of both living and extinct lineages within the teleost crown group, and several non-teleost ray-finned fishes. This sample allows us to estimate relative genome sizes in extinct groups, providing information on the absolute timing and specific phylogenetic position of the teleost WGD as well as the timescale of post-duplication reductions in genome size (24). Both statistical analysis and qualitative observations demonstrate the effectiveness of lacuna size for inferring large evolutionary increases in genome size: known polyploid lineages such as catostomids and salmonids, which underwent additional rounds of WGD, both show large osteocyte lacuna volumes compared to their close relatives (31).

Results

Our results suggest that WGD occurred early on the teleost stem lineage. Osteocyte lacuna volumes of early to mid-Mesozoic (Early Jurassic-Early Cretaceous) teleosts overlap with those of extant polyploid taxa and exceed values for non-polyploid taxa (Figs. 1-2, S1-3). Phylogenetic ancestral trait estimates attribute this to a substantial increase in lacuna volume (from 148 to 240 μm^3) immediately following the split of teleosts from holosteans, and therefore before the deepest-known divergences of the teleost total group (Fig. 1). The oldest stem-group teleosts in our sample with measurable lacuna volumes hail from the Early Jurassic (~195 Ma) and have large lacuna volumes similar to those of recent polyploids such as salmonids and catostomids (Fig. 2). Late Jurassic and Early Cretaceous members of the teleost crown-group generally also have large lacunae compared to extant teleosts. In contrast, late Mesozoic and Cenozoic teleosts mostly have lacuna volumes comparable to those of their closest modern relatives (Figs. 1–2, S1). Osteocyte lacuna volumes therefore decrease through time along the teleost stem-lineage, with further reductions within major lineages of crown teleosts (such as elopomorphs and clupeocephalans) or within some members of the stem group (such as ichthyodectiforms). Aspects of these patterns of lacuna size evolution are consistent with those inferred from molecular data. Nevertheless, our study provides valuable additional evidence, placing important constraints on the timing and phylogenetic placement of WGD on the extinct teleost stem lineage as a test of its relationship to phenotypic diversification.

Discussion

A large, almost two-fold increase in osteocyte sizes at the base of the teleost stem lineage suggests a phylogenetically-early occurrence of WGD. Large genome sizes can also occur via other genomic mechanisms such as the accumulation of transposable elements, introns, or tandem repeats (32–34) (e.g. within vertebrates, lungfishes and salamanders). Nevertheless, the timing, phylogenetic distribution (spanning early members of the teleost stem-lineage and their crown group), and observation of subsequent decreases in cell size all suggest that the patterns of genome size variation inferred here result from WGD and not from other forms of evolutionary genome size expansion. Furthermore, our previous work has demonstrated that polyploidy provides a strong statistical explanation for large osteocyte size in actinopterygians, on par with genome size (31).

The oldest stem-group teleosts in our sample (*Pholidophoroides* and *Pholidophoropsis*) are of Early Jurassic age. These taxa represent lineages that diverged much earlier from the teleost stem-group, and therefore constrain the timing of the teleost WGD to no later than the Late Triassic (~235 Ma) using phylogenetic ancestral state estimation (Fig. 1). Direct sampling of Triassic stem teleosts will provide a further test of this hypothesis (35), but this has not so far been possible in spite of multiple attempts, due to poor preservation of bone microstructure (*SI Appendix, Part II*). Our phylogenetically-inferred age for the teleost WGD falls within the timeframe estimated by some molecular studies (316-226 Ma (23); ~310 Ma (24)). The subsequent decrease in lacuna volumes toward the crown and within individual crown-group lineages indicates post-duplication genome-size reduction, spanning tens of millions of years. This confirms previous inferences of post-duplication genome size reduction based on clock analysis of paralogous genes,mathematical modelling, and the phylogenetic distribution of genome size in extant teleosts (24). Ichthyodectiforms, a long-lived clade of Mesozoic stem-teleosts, show a similar pattern of smaller volumes in more recent species compared to earlier ones, providing evidence of parallel reduction in an extinct lineage closely related to the crown (Fig. 1).

Our findings are inconsistent with hypotheses that propose that spectacular evolutionary diversification of teleosts is an immediate consequence of the WGD. Because of the phylogenetically-early occurrence of WGD, all currently recognized members of the teleost stem-

group have inferred duplicate genomes. Therefore, WGD did not coincide with the origin of celebrated teleost functional innovations like the mobile premaxilla, symmetrical caudal-fin and aspects of vertebral geometry implicated in their later evolutionary success (36, 37) (Fig. 1). These traits arose later — conceivably many millions of years after the inferred origin of WGD (35). WGD occurred during or before the Triassic, and therefore also predates more general phenotypic diversification, which occurred from the Late Jurassic onwards (38). The earliest known (i.e., Triassic and Early Jurassic) stem teleosts conform to a conservative bodyplan, being small, fusiform fishes with ganoid scales. Quantitative analyses show consistently low levels of morphological diversity for at least ~50 Myr after the origin of the teleost total-group (38). The conservative early history of teleosts cannot be attributed to inadequacies of the Triassic record, which yields an abundance of fish fossils (39) including anatomically diverse holosteans (38). The morphological diversity of teleosts increased only gradually in the later stages of the Mesozoic, especially in the Cretaceous with the origin of fundamentally new bodyplans (e.g., eel-like, deep-bodied (40, 41)) and amplified by prolific morphological diversification in the early Paleogene (42, 43). Triassic-Early Cretaceous teleosts, including early crown-group taxa, show comparable or lower rates of body-shape evolution than contemporary holosteans (18), which are known to lack duplicated genomes (20). Early teleosts also show delayed patterns of taxonomic and ecological diversification compared to the timing of WGD inferred here: teleosts comprise only a minority of actinopterygian genera in marine and freshwater settings throughout the Triassic (39) and much of the Jurassic (44), even after the origin of their crown-group. Only in the Late Jurassic — at least 80 Myr after the WGD — does the taxonomic diversity of teleosts approach or exceed that of other actinopterygians, as evidenced by the marine fossil assemblages of famous *Lagerstätten* like Cerin and Solnhofen (43).

This temporal pattern suggests an alternative hypothesis: that reorganization and integration of genomic architecture after the WGD, and not WGD itself, drove the phenotypic diversification and origin of key morphological traits during later stages of teleost evolution. Consistent with this hypothesis, the 50 Myr-interval between the origin of the teleost total-group and their observed increase in morphological diversity (38) is similar to the estimated duration of post-WGD genome size reductions to modern teleost-like levels (20)(Fig. 2). Decrease in genome size is associated with profound changes in genome organization, through gene loss, neo-functionalization, and changes in expression.

Because of recent focus on genomic hypotheses, relatively little attention has been given to alternative explanations for the phenomenal diversity of extant teleosts. However, the temporal incongruence between a Triassic WGD and the late Mesozoic and early Cenozoic events of teleost diversification (18, 38, 43) also demands broader consideration of non-genomic hypotheses. One possibility is that teleosts were the beneficiaries of biotic turnover during major environmental changes of the late Mesozoic. For example, the mid-Cretaceous interval saw substantial environmentally-driven alterations to marine ecosystems induced by large igneous province volcanism (45), regional ocean anoxic events (46), and other climatic variations. Among these, the Turonian thermal maximum c. 92 million years ago (47) was a major climate perturbation associated with biotic turnover at all levels of the marine trophic chain (46, 48). The early Late Cretaceous coincided with a major burst of cladogenesis in marine fishes, the diversity of which is strongly and positively correlated with sea surface temperature during the Jurassic and Cretaceous (44, 49). Although teleosts dominate this mid-Cretaceous radiation, other ray-finned fish groups show similar patterns (e.g., pycnodonts; (50)), arguing for a general—rather than clade-specific—mechanism. The Cretaceous concluded 66 million years ago with a major mass extinction event. This induced a major reorganization of aquatic ecosystems, particularly in higher trophic levels of marine environments (51, 52). Paleontological and molecular data indicate major morphological diversification among marine teleosts in the early Paleogene (42, 53). This was associated with the colonization of different environments and the refilling of vacated functional roles (54–57), and included short-lived “evolutionary experiments” found alongside familiar living lineages (58, 59). As with the mid-Cretaceous, the early Paleocene represented a

"hothouse" period in Earth's climate history, with evidence that higher temperatures might have led to increased fish production in some marine settings (60). Collectively, these observations suggest a role for environmental change and ecosystem reorganization in facilitating the diversification of teleosts, either in addition to or instead of the effects from WGD.

Our results provide direct fossil evidence of phylogenetic placement of the teleost WGD, and a more robust window for the timing and consequences of teleost genome duplication. WGD occurred early on the teleost stem-lineage, with considerable time for post-duplication reorganizations of genomic architecture before the morphological and taxonomic radiation of teleosts. This suggests an indirect and temporally-offset link between WGD and evolutionary diversification, if any, and is consistent with genomic studies of recent polyploids among fishes (e.g. salmonids (9)) and vascular plants (10). More broadly, our data demonstrate the potential of the fossil record of cell structures (26) as an independent source of evidence on genomic events that may have underpinned major diversification events, not just in fishes and other vertebrates, but also in plants and across the Tree of Life (2, 3).

Materials and Methods

- **Specimen collection**

Our taxon sample builds on a previous study (31) that collected osteocyte lacuna volumes for 34 species of extant actinopterygians (including 28 teleost species). The present study adds 61 fossil species displaying osteocytic bone (61) to this sample: 8 non-teleost actinopterygians, 26 stem-group teleosts, and 27 crown teleosts. They range from 2.5 (Pliocene) to 252 (Early Triassic) million years in age (*SI Appendix, Part I*, Dataset S1). However, no representative of the teleost lineage is older than 200 million years (Early Jurassic; *SI Appendix, Part II*). As fossil specimens have a higher density than extant ones, capturing a decent signal of transmitted X-ray beam could be challenging should the specimens be too large. Thus, we took small (~ 1-5 mm) bone samples from the fossils, targeting areas that reduced the loss of anatomical information from the specimens (e.g., areas affected by pre-existing cracks or broken bone). Since lacunae vary in volume from one bone to another (30, 31), the same skeletal element has to be used consistently across the sample. Therefore, all samples were taken from the dentary bone (lower jaw) as it is found in all target taxa and is often preserved in the fossil record. Moreover, the already-existing dataset of extant actinopterygians (31), used dentary bones for each included species.

- **Data acquisition**

The data presented in this study were acquired using propagation phase contrast synchrotron radiation X-ray micro-computed tomography (PPC-SRμCT). Acquisition was performed over the course of three sessions in two synchrotrons: two sessions were done at the ID19 beamline of the European Synchrotron Radiation Facility (ESRF, Grenoble, France) and the remaining session was done at the I13-2 Diamond Manchester Imaging beamline of the Diamond Light Source (DLS, Didcot, UK). The setups on the two beamlines were generally similar, the main difference being that much higher energies were available at the ID19 beamline (up to 112 keV in this study) compared to I13-2 beamline (here, 21.39 keV). Both setups produced high-resolution data, with recorded voxel sizes of 0.357 μm at the I13-2 beamline and near 0.7 μm at the ID19 beamline. A voxel size of 0.7 μm or smaller is empirically adequate for imaging osteocyte lacunae (31, 62–64). Detailed information on the synchrotron experimental setups is found in the *SI Appendix, Part III* and Dataset S2. The tomograms (digital 'slices') obtained from our specimens were processed with the software VGSTUDIO MAX v. 3.0 and 3.1 (Volume Graphics, Heidelberg, Germany), to segment osteocyte lacunae from the fossil bone matrix. We used specimen-specific grey-value thresholds to segment osteocyte lacunae from a selected region of interest, focusing on well-defined lacunae from primary bone, excluding objects such as specimen edges, cracks and abiotic inclusions manually. Grey-value thresholds were selected to ensure that the boundaries of segmented osteocytes coincided with the boundaries of osteocytes in the image

volume, attempting to maximize fit of the segmented object to the underlying data. We did not segment the canaliculi that accommodate cytoplasmic projections of the osteocytes, as they were not visible in every tomogram and thus could bias our estimates of the osteocyte lacuna volumes. We used the 'Porosity/Inclusion' module of VGSTUDIO MAX, to measure the individual lacuna volumes. This module also provides visualization, coloring lacunae according to their volume with a consistent color range across our sample (Figs. 1-2, S1). We analyzed median osteocyte volumes computed from the entire population of segmented objects, excluding objects smaller than 25 μm^3, which did not generally represent osteocyte lacunae. The whole protocol followed the one we applied previously for extant actinopterygians (31), allowing us to incorporate extant and fossil samples together in downstream analyses. The complete measurement and positional data for populations of osteocyte lacunae in all specimens analyzed are available in Dryad (https://doi.org/10.5061/dryad.bcc2fqzcc), and our scan image volumes are available on MorphoSource (https://www.morphosource.org/projects/0000C1125).

We used objective quality control criteria to exclude some specimens from the analysis after obtaining PPC-SRμCT tomograms (*SI Appendix, Part I.3*). Datasets were excluded based on the following criteria: [1] When the data clearly showed the absence of osteocyte lacunae from the sample, either because the taxon has anosteocytic bone (61, 65), or because osteocytes were not fossilized. [2] When osteocyte lacunae were present but not sufficiently well-resolved to allow an accurate segmenting of the lacunae or measurement of their volume. [3] After segmenting the osteocyte lacunae, we excluded more specimens in which the number of osteocyte lacunae we were able to measure was too small to warrant confident estimates of average size (n<~50). Prior to the segmentation and measurement, our sample of tomograms included 77 fossil specimens in total representing 71 species, and notably included five stem-group teleosts from the Triassic. Of these, 16 specimens were excluded based on quality control criteria (see the *SI Appendix, Part I.1 and I.2* for the complete list of specimens).

- **Reference tree**

We used a composite phylogeny based on a consensus of published hypotheses on the interrelationships of fossil actinopterygians, and divergence ages inferred from earliest known occurrences in the fossil record (*SI Appendix, Part I.2*, Dataset S1). The framework for extant taxa is a recently published molecular timetree (66) that has the best species sample and taxonomic coverage of any actinopterygian phylogeny so far published. Fossil taxa were stitched to the resulting tree using a custom script that makes extensive use of the R package ape version 5.0 (67) and is available in Dryad (https://doi.org/10.5061/dryad.bcc2fqzcc). Fossil age ranges, specifier taxa for their sister clades, and minimum divergence times from those sister clades based on fossil occurrences are available as Dataset S1. Phylogenetic position and age data for the fossil taxa and their divergence times from other species were taken from the most recent available paleontological and stratigraphic information (see the *SI Appendix, Part I.2* for the justification of phylogenetic and stratigraphic placement for each species in the sample). Extant terminals were pruned, retaining the 34 extant species for which we measured osteocyte volumes, prior to analysis. The resulting tree is available as Fig. S1 and Dataset S3.

- **Data analysis**

To visualize patterns of genome size evolution, we mapped osteocyte lacuna volume (Dataset S4) to our composite phylogeny with branch lengths of units in time, using ancestral character state estimation (68) via the ace function of ape version 5.0 (67). Osteocyte lacuna volume was $\log_{10}$-transformed prior to analysis and is used as a proxy for genome size (31). WGD predicts an approximate doubling of osteocyte size somewhere on the teleost stem-lineage.

Data availability

The SRμCT data (tomograms and 3D reconstructions) generated during this study have been deposited online in MorphoSource: www.morphosource.org/projects/0000C1125 (fossil specimens) and www.morphosource.org/projects/00000C959 (extant specimens). The median

osteocyte lacuna volumes for each specimen are available in Dataset S4. The complete volume measurement data for populations of osteocyte lacunae in all specimen analysed, as well as the custom R script used to build the reference tree and reconstruct osteocyte lacuna volume evolution are available in Dryad (https://doi.org/10.5061/dryad.bcc2fqzcc). All other data files are included in the SI Appendix and Datasets S1-S4.

Acknowledgments

This research was supported by the Leverhulme Trust (RPG-2016-168) and by a Junior Research Fellowship at Wolfson College, University of Oxford. Beamtime was allocated thanks to three proposals accepted by the European Synchrotron Radiation Facility (LS 2614, LS 2758) and the Diamond Light Source (MG 21817). P. Tafforeau, M. Storm and M.C. Zdora are thanked for their technical help and advice during the synchrotron experiments. We thank members of the Oxford Clay Working Group, including C. Nicklin, M. Wildman, H. Middleton and S. Moore-Faye for specimens used as pilot data. The authors thank E. Bernard, Z. Johanson, M. Richter, G. Clément, H. Ketchum, C. Klug, A. Lopez-Arbarello, A. Folie, M. Valle, A. Paganoni, M. Malzanni, A. Aiello and F. Witzmann for providing access to collection specimens and allowing us to sample them.

References

1. Y. Van De Peer, S. Maere, A. Meyer, The evolutionary significance of ancient genome duplications. *Nat. Rev. Genet.* **10**, 725–732 (2009).

2. J. W. Clark, P. C. J. Donoghue, Whole-genome duplication and plant macroevolution. *Trends Plant Sci.* **23**, 933–945 (2018).

3. O. Simakov, *et al.*, Deeply conserved synteny resolves early events in vertebrate evolution. *Nat. Ecol. Evol.* (2020) https:/doi.org/10.1038/s41559-020-1156-z.

4. S. Ohno, *Evolution by Gene Duplication* (Springer, 1970).

5. K. D. Crow, G. P. Wagner, What is the role of genome duplication in the evolution of complexity and diversity? *Mol. Biol. Evol.* **23**, 887–892 (2006).

6. S. M. K. Glasauer, S. C. F. Neuhauss, Whole-genome duplication in teleost fishes and its evolutionary consequences. *Mol. Genet. Genomics* **289**, 1045–1060 (2014).

7. F. Santini, L. J. Harmon, G. Carnevale, M. E. Alfaro, Did genome duplication drive the origin of teleosts? A comparative study of diversification in ray-finned fishes. *BMC Evol. Biol.* **9**, 194 (2009).

8. R. Ren, *et al.*, Widespread whole genome duplications contribute to genome complexity and species diversity in angiosperms. *Mol. Plant* **11**, 414–428 (2018).

9. D. J. Macqueen, I. A. Johnston, A well-constrained estimate for the timing of the salmonid whole genome duplication reveals major decoupling from species diversification. *Proc. R. Soc. B Biol. Sci.* **281**, 20132881 (2014).

10. I. Mayrose, *et al.*, Recently formed polyploid plants diversify at lower rates. *Science (80-.).* **333**, 1257–1257 (2011).

11. V. Ravi, B. Venkatesh, Rapidly evolving fish genomes and teleost diversity. *Curr. Opin. Genet. Dev.* **18**, 544–550 (2008).

12. V. Ravi, B. Venkatesh, The divergent genomes of teleosts. *Annu. Rev. Anim. Biosci.* **6**, 47–68 (2018).

13. T. Desvignes, J. Sydes, J. Montfort, J. Bobe, J. H. Postlethwait, Evolution after whole genome duplication: teleost microRNAs. *Mol. Biol. Evol.*, 0–2 (2021).

14. E. M. Smith, T. R. Gregory, Patterns of genome size diversity in the ray-finned fishes. *Hydrobiologia* **625**, 1–25 (2009).

15. R. A. Leggatt, G. K. Iwama, Occurrence of polyploidy in the fishes. *Rev. Fish Biol. Fish.* **13**, 237–246 (2003).

16. A. Amores, *et al.*, Zebrafish *hox* clusters and vertebrate genome evolution. *Science (80-.).* **282**, 1711–1714 (1998).

17. C. Berthelot, *et al.*, The rainbow trout genome provides novel insights into evolution after whole-genome duplication in vertebrates. *Nat. Commun.* **5**, 3657 (2014).

18. J. T. Clarke, G. T. Lloyd, M. Friedman, Little evidence for enhanced phenotypic evolution in early teleosts relative to their living fossil sister group. *Proc. Natl. Acad. Sci.* **113**, 11531–11536 (2016).

19. J. S. Taylor, I. Braasch, T. Frickey, A. Meyer, Y. Van de Peer, Genome duplication, a trait shared by 22,000 species of ray-finned fish. *Genome Res.* **13**, 382–390 (2003).

20. I. Braasch, *et al.*, The spotted gar genome illuminates vertebrate evolution and facilitates human-teleost comparisons. *Nat. Genet.* **48**, 427–437 (2016).

21. M. Friedman, The early evolution of ray-finned fishes. *Palaeontology* **58**, 213–228 (2015).

22. G. Arratia, “The Jurassic and the early history of teleosts” in *Mesozoic Fishes - Systematics and Paleoecology*, G. Arratia, G. Viohl, Eds. (Verlag Dr. Friedriech Pfeil, 1996), pp. 243–259.

23. I. A. Hurley, *et al.*, A new time-scale for ray-finned fish evolution. *Proc. R. Soc. B Biol. Sci.* **274**, 489–498 (2007).

24. J. Inoue, Y. Sato, R. Sinclair, K. Tsukamoto, M. Nishida, Rapid genome reshaping by multiple-gene loss after whole-genome duplication in teleost fish suggested by mathematical modeling. *Proc. Natl. Acad. Sci.* **112**, 14918–14923 (2015).

25. C. L. Organ, A. M. Shedlock, A. Meade, M. Pagel, S. V. Edwards, Origin of avian genome size and structure in non-avian dinosaurs. *Nature* **446**, 180–184 (2007).

26. P. C. J. Donoghue, Fossil cells. *Curr. Biol.* **30**, R485–R490 (2020).

27. C. L. Organ, A. Canoville, R. R. Reisz, M. Laurin, Paleogenomic data suggest mammal-like genome size in the ancestral amniote and derived large genome size in amphibians. *J. Evol. Biol.* **24**, 372–380 (2011).

28. T. Cavalier-Smith, Skeletal DNA and the evolution of genome size. *Annu. Rev. Biophys. Bioeng.* **11**, 273–302 (1982).

29. E. Olmo, Nucleotype and cell size in vertebrates: a review. *Basic Appl. Histochem.* **27**, 227–256 (1983).

30. M. D. D'Emic, R. B. J. Benson, Measurement, variation, and scaling of osteocyte lacunae: a case study in birds. *Bone* **57**, 300–310 (2013).

31. D. Davesne, A. D. Schmitt, V. Fernandez, R. B. J. Benson, S. Sanchez, Three-dimensional characterisation of osteocyte volumes at multiple scales, and its relationship with bone biology and genome evolution in ray-finned fishes. *J. Evol. Biol.* **33**, 808–830 (2020).

32. T. Lefébure, *et al.*, Less effective selection leads to larger genomes. *Genome Res.* **27**, 1016–1028 (2017).

33. H. C. Liedtke, D. J. Gower, M. Wilkinson, I. Gomez-Mestre, Macroevolutionary shift in the size of amphibian genomes and the role of life history and climate. *Nat. Ecol. Evol.* **2**, 1792–1799 (2018).

34. A. Kapusta, A. Suh, C. Feschotte, Dynamics of genome size evolution in birds and mammals. *Proc. Natl. Acad. Sci.*, 201616702 (2017).

35. G. Arratia, Morphology, taxonomy, and phylogeny of Triassic pholidophorid fishes (Actinopterygii, Teleostei). *J. Vertebr. Paleontol.* **33**, 1–138 (2013).

36. B. Schaeffer, D. E. Rosen, Major adaptive levels in the evolution of the actinopterygian feeding mechanism. *Am. Zool.* **1**, 187–204 (1961).

37. L. Sallan, Evolution: Spinal innovation enabled by genome duplication. *Curr. Biol.* **30**, R1006–R1008 (2020).

38. J. T. Clarke, M. Friedman, Body-shape diversity in Triassic–Early Cretaceous neopterygian fishes: sustained holostean disparity and predominantly gradual increases in teleost phenotypic variety. *Paleobiology* **44**, 402–433 (2018).

39. C. Romano, *et al.*, Permian-Triassic Osteichthyes (bony fishes): diversity dynamics and body size evolution. *Biol. Rev.* **91**, 106–147 (2016).

40. J. G. Maisey, *Santana Fossils: an Illustrated Atlas*, J. G. Maisey, Ed. (T.F.H., 1991).

41. P. L. Forey, L. Yi, C. Patterson, C. E. Davies, Fossil fishes from the Cenomanian (Upper Cretaceous) of Namoura, Lebanon. *J. Syst. Palaeontol.* **1**, 227–330 (2003).

42. M. Friedman, Explosive morphological diversification of spiny-finned teleost fishes in the aftermath of the end-Cretaceous extinction. *Proc. R. Soc. B Biol. Sci.* **277**, 1675–1683 (2010).

43. G. Guinot, L. Cavin, 'Fish' (Actinopterygii and Elasmobranchii) diversification patterns through deep time. *Biol. Rev.* **91**, 950–981 (2016).

44. L. Cavin, P. L. Forey, C. Lécuyer, Correlation between environment and Late Mesozoic ray-finned fish evolution. *Palaeogeogr. Palaeoclimatol. Palaeoecol.* **245**, 353–367 (2007).

45. S. E. Bryan, *et al.*, The largest volcanic eruptions on Earth. *Earth-Science Rev.* **102**, 207–229 (2010).

46. R. M. Leckie, T. J. Bralower, R. Cashman, Oceanic anoxic events and plankton evolution: biotic response to tectonic forcing during the mid-Cretaceous. *Paleoceanography* **17**, 1–29 (2002).

47. C. Linnert, *et al.*, Evidence for global cooling in the Late Cretaceous. *Nat. Commun.* **5**, 4194 (2014).

48. V. Fischer, N. Bardet, R. B. J. Benson, M. S. Arkhangelsky, M. Friedman, Extinction of fish-shaped marine reptiles associated with reduced evolutionary rates and global environmental volatility. *Nat. Commun.* **7**, 10825 (2016).

49. G. Guinot, L. Cavin, Distinct responses of elasmobranchs and ray-finned fishes to long-term global change. *Front. Ecol. Evol.* **7**, 513 (2020).

50. J. J. Cawley, *et al.*, Rise and fall of †Pycnodontiformes: Diversity, competition and extinction of a successful fish clade. *Ecol. Evol.* (2021) https:/doi.org/10.1002/ece3.7168.

51. N. Bardet, Extinction events among Mesozoic marine reptiles. *Hist. Biol.* **7**, 313–324 (1994).

52. M. Friedman, Ecomorphological selectivity among marine teleost fishes during the end-Cretaceous extinction. *Proc. Natl. Acad. Sci.* **106**, 5218–5223 (2009).

53. E. C. Sibert, R. D. Norris, New Age of Fishes initiated by the Cretaceous-Paleogene mass extinction. *Proc. Natl. Acad. Sci.* **112**, 8537–8542 (2015).

54. E. Ribeiro, A. M. Davis, R. A. Rivero-Vega, G. Ortí, R. Betancur, Post-Cretaceous bursts of evolution along the benthic-pelagic axis in marine fishes. *Proc. R. Soc. B Biol. Sci.* **285**, 20182010 (2018).

55. M. Friedman, *et al.*, A phylogenomic framework for pelagiarian fishes (Acanthomorpha: Percomorpha) highlights mosaic radiation in the open ocean. *Proc. R. Soc. B Biol. Sci.* **286**, 20191502 (2019).

56. D. R. Bellwood, C. H. R. Goatley, O. Bellwood, The evolution of fishes and corals on reefs: form, function and interdependence. *Biol. Rev.* **92**, 878–901 (2017).

57. S. A. Price, *et al.*, Two waves of colonization straddling the K-Pg boundary formed the modern reef fish fauna. *Proc. R. Soc. B Biol. Sci.* **281**, 20140321 (2014).

58. D. Davesne, G. Carnevale, M. Friedman, *Bajaichthys elegans* from the Eocene of Bolca (Italy) and the overlooked morphological diversity of Zeiformes (Teleostei, Acanthomorpha). *Palaeontology* **60**, 255–268 (2017).

59. A. Capobianco, *et al.*, Large-bodied sabre-toothed anchovies reveal unanticipated ecological diversity in early Palaeogene teleosts. *R. Soc. Open Sci.* **7**, 192260 (2020).

60. G. L. Britten, E. C. Sibert, Enhanced fish production during a period of extreme global warmth. *Nat. Commun.* **11**, 1–6 (2020).

61. D. Davesne, *et al.*, The phylogenetic origin and evolution of acellular bone in teleost fishes: insights into osteocyte function in bone metabolism. *Biol. Rev.* **94**, 1338–1363 (2019).

62. S. Sanchez, *et al.*, 3D microstructural architecture of muscle attachments in extant and fossil vertebrates revealed by synchrotron microtomography. *PLoS One* **8**, e56992 (2013).

63. S. Sanchez, P. Tafforeau, P. E. Ahlberg, The humerus of *Eusthenopteron*: a puzzling organization presaging the establishment of tetrapod limb bone marrow. *Proc. R. Soc. B Biol. Sci.* **281**, 20140299 (2014).

64. S. Sanchez, P. E. Ahlberg, K. M. Trinajstic, A. Mirone, P. Tafforeau, Three-dimensional synchrotron virtual paleohistology: a new insight into the world of fossil bone microstructures. *Microsc. Microanal.* **18**, 1095–1105 (2012).

65. D. Davesne, F. J. Meunier, M. Friedman, R. B. J. Benson, O. Otero, Histology of the endothermic opah (*Lampris* sp.) suggests a new structure–function relationship in teleost fish bone. *Biol. Lett.* **14**, 20180270 (2018).

66. D. L. Rabosky, *et al.*, An inverse latitudinal gradient in speciation rate for marine fishes. *Nature* **559**, 392–395 (2018).

67. E. Paradis, K. Schliep, ape 5.0: an environment for modern phylogenetics and evolutionary analyses in R. *Bioinformatics* **35**, 526–528 (2019).

68. D. Schluter, T. Price, A. Ø. Mooers, D. Ludwig, Likelihood of ancestor states in adaptive radiation. *Evolution (N. Y).* **51**, 1699–1711 (1997).

Figures

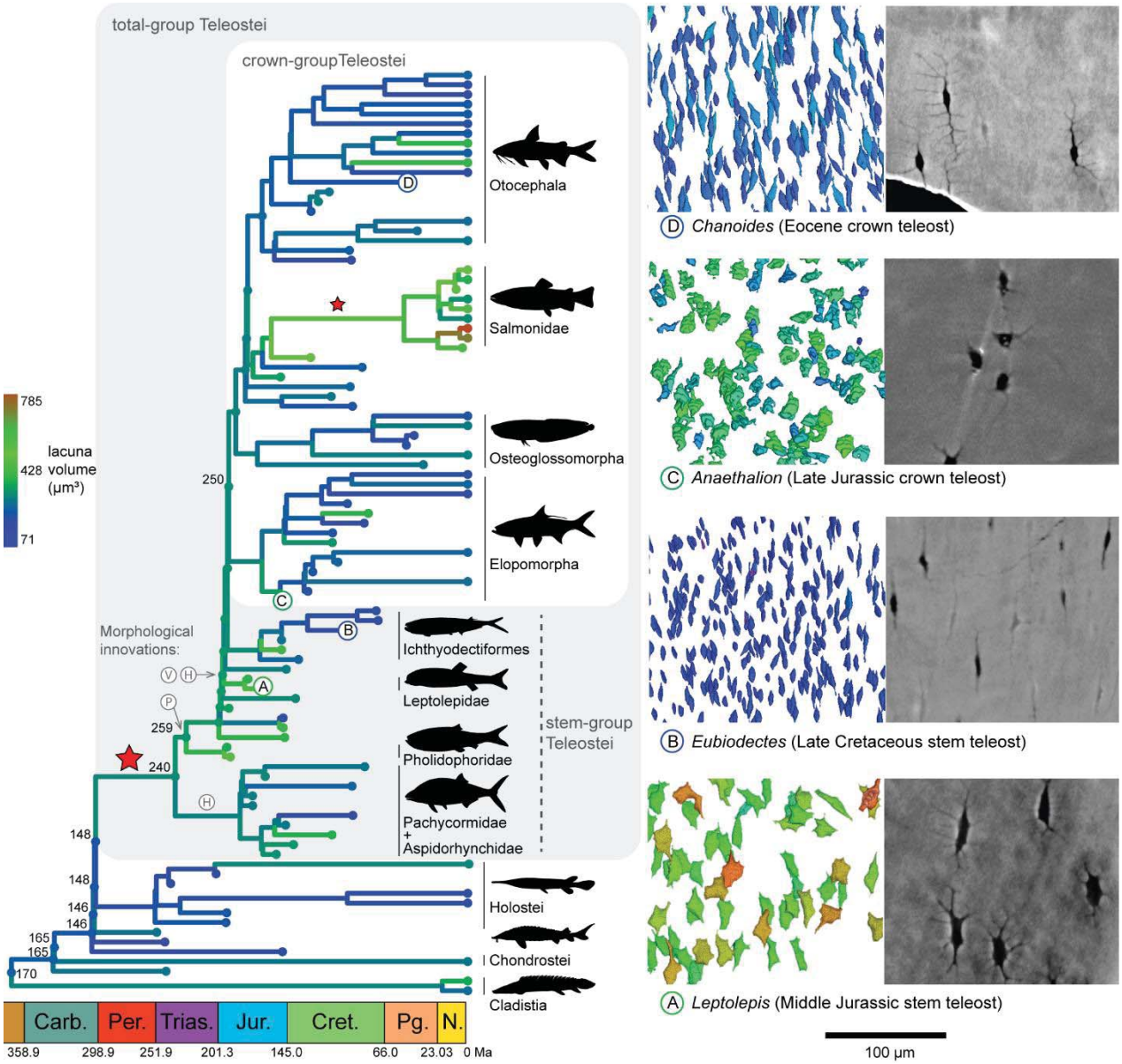

Figure 1. Evolution of osteocyte lacuna volume in fossil and modern teleosts revealed by synchrotron microtomography. Timescaled composite phylogeny of actinopterygians with mapped cell-size volumes for fossil and modern lineages. Red stars visualise the inferred occurrences of whole-genome duplications: the teleost WGD (large star), and the salmonid-specific WGD (small star). Renderings of osteocyte lacunae shown for highlighted fossil taxa branching close in time to the inferred teleost-specific WGD (A, C) and those substantially postdating it (B, D). Letters correspond to key teleost synapomorphies, mapped to the corresponding node based on morphological phylogeny (35): P, mobile premaxilla; H, homocercal caudal fin; A, vertebral autocentra.

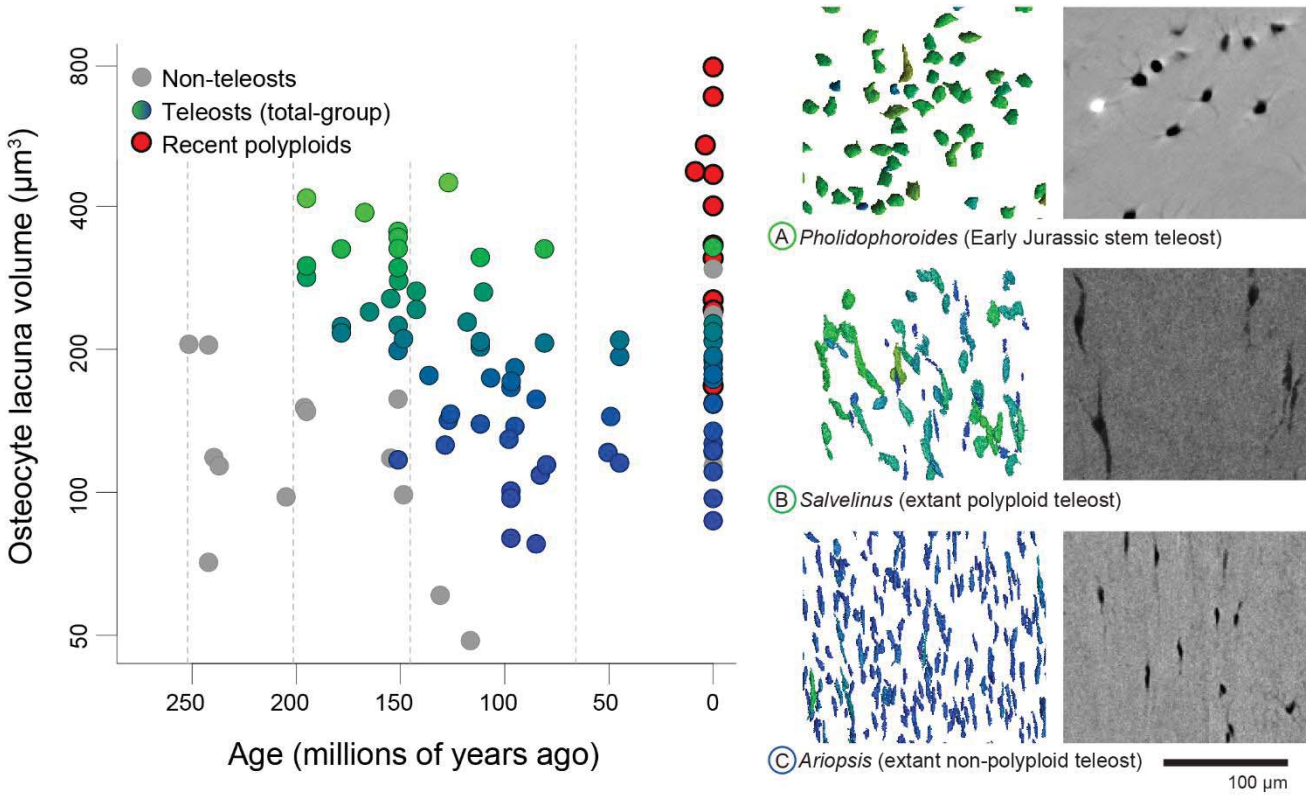

547

548 **Figure 2. Evolution of osteocyte lacuna volume in fossil and modern teleosts revealed by**
549 **synchrotron microtomography, plotted against time.** We show cell size in an Early Jurassic
550 stem-group teleost (A), within the range of modern polyploid species (exemplified by the salmonid
551 *Salvelinus*; B), and indicative of a WGD. A steady decrease in cell size through time is evident in
552 the fossil record, and is reflected by the relatively small cells of many extant teleosts, which lack
553 polyploidy events subsequent to the ancestral teleost WGD (e.g. the catfish *Ariopsis*; C). Note
554 semi-log axes (osteocyte lacuna volume values are log-transformed). Color scale follows Fig. 1.

555

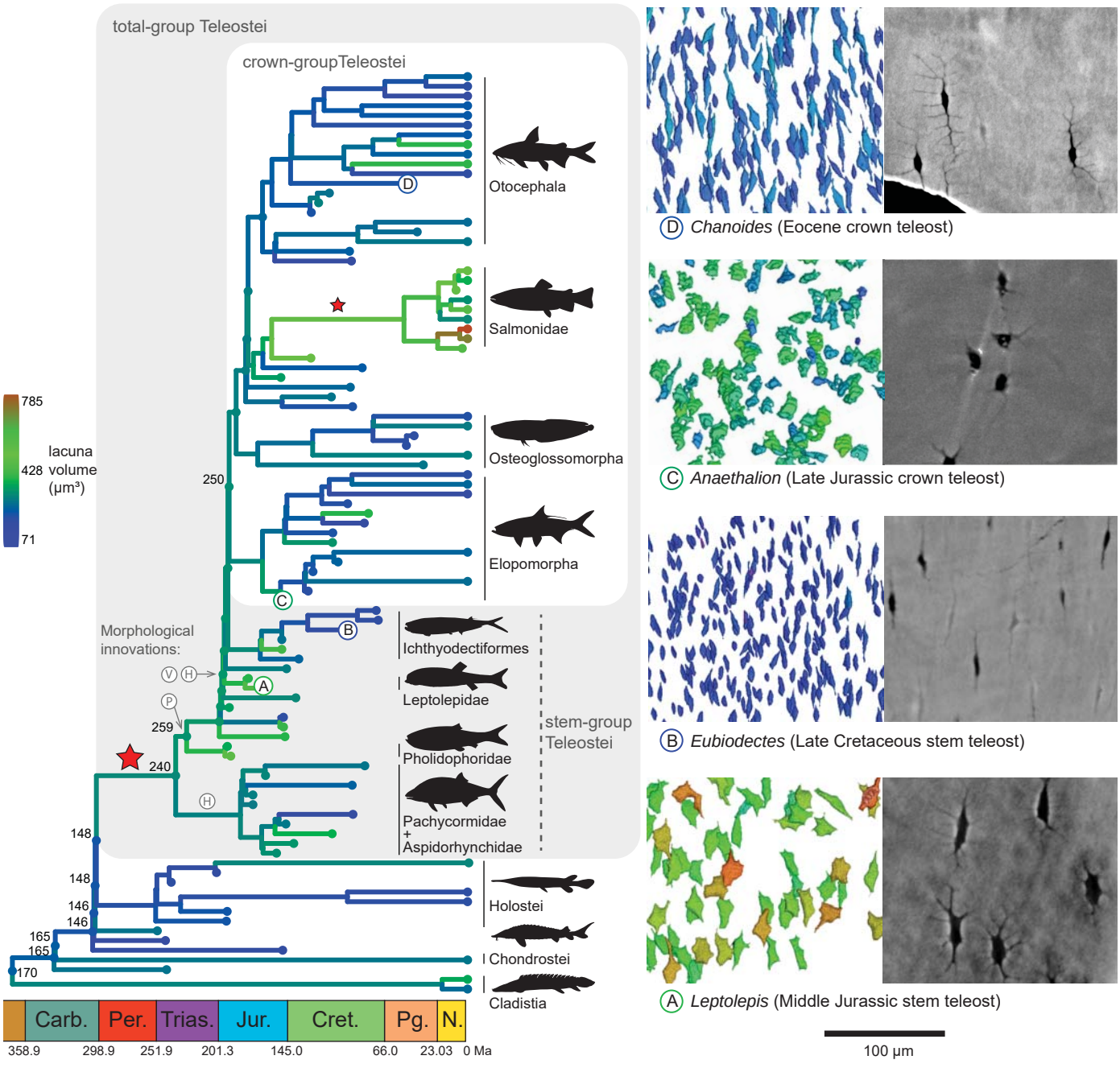
total-group Teleostei
crown-groupTeleostei
Otocephala
Salmonidae
Osteoglossomorpha
Elopomorpha
Ichthyodectiformes
Leptolepidae
Pholidophoridae
Pachycormidae
+
Aspidorhynchidae
stem-group
Teleostei
Holostei
Chondrostei
Cladistia
Morphological
innovations:
V
H
P
A
B
C
D
785
428
71
lacuna
volume
(µm³)
250
259
240
148
148
146
146
165
165
170
Carb.
Per.
Trias.
Jur.
Cret.
Pg.
N.
358.9
298.9
251.9
201.3
145.0
66.0
23.03
0 Ma
D Chanoides (Eocene crown teleost)
C Anaethalion (Late Jurassic crown teleost)
B Eubiodectes (Late Cretaceous stem teleost)
A Leptolepis (Middle Jurassic stem teleost)
100 µm

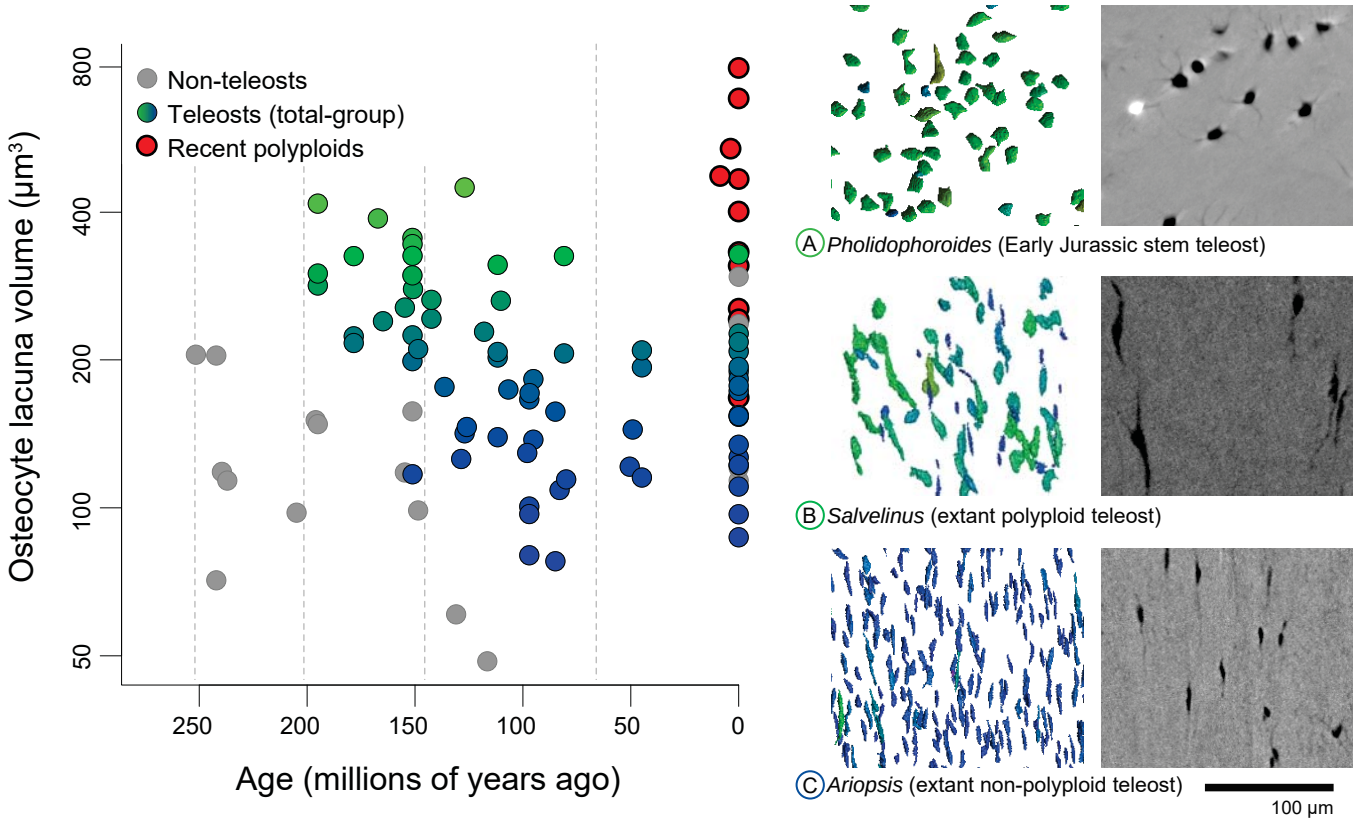
Non-teleosts
Teleosts (total-group)
Recent polyploids
Osteocyte lacuna volume (µm³)
800
400
200
100
50
250
200
150
100
50
0
Age (millions of years ago)
A Pholidophoroides (Early Jurassic stem teleost)
B Salvelinus (extant polyploid teleost)
C Ariopsis (extant non-polyploid teleost)
100 µm

PNAS
www.pnas.org

Supplementary Information for

Fossilized cell structures identify an ancient origin for the teleost whole-genome duplication.

Donald Davesne[1,2,3*], Matt Friedman[4], Armin D. Schmitt[1,5], Vincent Fernandez[6,7], Giorgio Carnevale[8], Per E. Ahlberg[9], Sophie Sanchez[6,9], Roger B. J. Benson[1,*]

[1]Department of Earth Sciences, University of Oxford, Oxford, UK
[2]Institut de Systématique, Évolution, Biodiversité, UMR 7205 (MNHN – Sorbonne Université – CNRS – EPHE), Muséum national d'Histoire naturelle, Paris, France
[3]Museum für Naturkunde, Leibniz-Institut für Evolutions- und Biodiversitätsforschung, Berlin, Germany
[4]Museum of Paleontology and Department of Earth and Environmental Sciences, University of Michigan, Ann Arbor, USA
[5]Department of Earth Sciences, University of Cambridge, Cambridge, UK
[6]European Synchrotron Radiation Facility, Grenoble, France
[7]Imaging and Analysis Centre, Natural History Museum, London, UK
[8]Dipartimento di Scienze della Terra, Università degli Studi di Torino, Turin, Italy
[9]Subdepartment of Evolution and Development, Department of Organismal Biology, Uppsala University, Uppsala, Sweden

*Corresponding authors: Donald Davesne and Roger B. J. Benson.
Email: donald.davesne@gmail.com; roger.benson@earth.ox.ac.uk

This PDF file includes:

Supplementary text
Figures S1 to S3
Legends for Datasets S1 to S3
SI References

Other supplementary materials for this manuscript include the following:

Datasets S1 to S3

Supplementary Information Text

I. Complete list of specimens used in the study

This list includes all fossil specimens that we SRμCT-scanned for the present study. Some of the specimens were not included in the downstream analysis because they did not yield exploitable data in the form of osteocyte lacuna volumes.

I.1. Institutional abbreviations for fossil specimens

IRSNB – Institut Royal des Sciences Naturelles de Belgique, Brussels, Belgium; MB.f – Museum für Naturkunde, Berlin, Germany; MCSNB – Museo Civico di Scienze Naturali, Bergamo, Italy; MNHN – Muséum National d'Histoire Naturelle, Paris, France; NHMUK – Natural History Museum, London, UK; OUMNH – Oxford University Museum of Natural History, Oxford, UK; PIMUZ – Paläontologisches Institut und Museum, Zurich, Switzerland; UMMP – University of Michigan Museum of Paleontology, Ann Arbor, USA.

I.2. Justification of the phylogenetic and stratigraphic placement of the fossil species used in the analyses

We used the Rabosky *et al.* (1) phylogeny as our reference tree for extant taxa, since it was the most complete molecular tree of actinopterygians available at the date of our study. Moreover, it provides estimates of divergence times that are amongst the closest to what is suggested by the fossil record (i.e. 192 Ma for the origin of crown-group teleosts).

- †*Paleolox larsoni* Kimmel, 1975
Specimen number: UMMP V74157
Position: stem-group *Salvelinus* according to (2, 3)
Position in the reference tree: sister to the clade (crown *Salvelinus*) comprising *Salvelinus leucomaenis leucomaenis*, *Salvelinus confluentus*, their most recent common ancestor and all its descendants
Age / Locality: Miocene / Chalk Hills Formation, USA – 9.8-7.4 Ma (2, 4)
Minimum divergence time: †*Paleolox larsoni* itself is the oldest representative of the total-group *Salvelinus*.

- †*Prosopium prolixus* Smith, 1975
Specimen number: UMMP 21728
Position: in total-group *Prosopium* according to (2)
Position in the reference tree: sister to the clade (crown *Prosopium*) comprising *Prosopium coulterii*, *Prosopium spilonotus*, their most recent common ancestor and all its descendants
Age / Locality: Pliocene / Glenns Ferry Formation, USA – 5.0-2.5 Ma (2, 4)
Minimum divergence time: †*P. prolixus* itself is the oldest representative of the total-group *Prosopium*.

- †*Spaniodon elongatus* Pictet, 1850
Specimen number: NHMUK PV OR 44831
Position: crown Euteleostei, sister to "Osmeroidei" (i.e. Osmeriformes in the reference phylogeny) according to (5)
Position in the reference tree: sister to the clade (crown Osmeriformes) comprising *Retropinna retropinna*, *Osmerus eperlanus*, their most recent common ancestor and all its descendants

Age / Locality: Late Santonian / Sahel Alma, Lebanon – 86.3-83.6 Ma (6, 7)
Minimum divergence time: †*Spaniodon* itself is the oldest representative of the total-group Osmeriformes.

- †*Pattersonella formosa* (Traquair, 1908)
Specimen number: IRSNB Vert-01680-00240 ce
Position: crown Euteleostei, is an "argentinoid" (i.e. Argentiniformes in the reference phylogeny) according to (8)
Position in the reference tree: sister to the clade (crown Argentiniformes) comprising *Argentina silus, Bathylagus antarcticus*, their most recent common ancestor and all its descendants
Age / Locality: Barremian-Aptian / Bernissart, Belgium – 128.0-126.0 Ma (9, 10)
Minimum divergence time: †*Pattersonella* itself is the oldest representative of the total-group Argentiniformes.

- †*Leptolepides sprattiformis* (Blainville, 1818)
Specimen number: MB.f.18203
Position: total-group Euteleostei according to (11–14)
Position in the reference tree: sister to the clade (crown Euteleostei) comprising *Lepidogalaxias salamandroides, Oncorhynchus mykiss*, their most recent common ancestor and all its descendants
Age / Locality: Kimmeridgian-Tithonian / Solnhofen Limestone, Germany - 150.94 Ma (15)
Minimum divergence time: †*Leptolepides* itself is the oldest representative of the total-group Euteleostei.

- †*Chanoides macropoma* Agassiz, 1843
Specimen number: NHMUK PV P 37226
Position: stem Otophysi according to (16, 17)
Position in the reference tree: sister to the clade (crown Otophysi) comprising *Gymnotus carapo, Danio rerio,* their most recent common ancestor and all its descendants
Age / Locality: late Ypresian / Bolca, Italy – 49.11 Ma (15)
Minimum divergence time: †*Santanichthys diasi*, oldest representative of the total-group Otophysi, probably within the clade formed by †*Chanoides* and crown Otophysi – 113.4-110 Ma (18).

- †*Tharrias araripis* Jordan & Branner, 1908
Specimen number: NHMUK PV P 54675b
Position: stem Chanidae (crown Gonorhynchiformes), sister to *Chanos chanos* according to (10)
Position in the reference tree: sister to *Chanos chanos*
Age / Locality: early Albian / Romualdo Member of the Santana Formation, Brazil – 113.4-110 Ma (10)
Minimum divergence time: †*Tharrias* itself is the oldest representative of the clade it forms with *Chanos*.

- †*Dastilbe elongatus* Silva-Santos, 1947
Specimen number: NHMUK PV P 63381
Position: stem Chanidae (crown Gonorhynchiformes), sister to [†*Tharrias* + *Chanos*] according to (10)
Position in the reference tree: sister to the clade comprising †*Tharrias araripes, Chanos chanos,* their most recent common ancestor and all its descendants
Age / Locality: late Aptian / Nova Olinda Member of the Crato Formation, Brazil – 123.0-113.0 Ma (10)
Minimum divergence time: †*Dastilbe* itself is the oldest representative of the clade it forms with †*Tharrias* and *Chanos*.

- †*Aethalionopsis robustus* (Traquair, 1911)
Specimen number: IRSNB Vert-01680-00556

Position: stem Chanidae (crown Gonorhynchiformes), sister to [†*Dastilbe* + †*Tharrias* + *Chanos*] according to (10, 19)
Position in the reference tree: sister to the clade comprising †*Dastilbe elongatus, Chanos chanos,* their most recent common ancestor and all its descendants
Age / Locality: Barremian-Aptian / Bernissart, Belgium – 128.0-126.0 Ma (9, 10)
Minimum divergence time: †*Aethalionopsis* itself is the oldest representative of the clade it forms with †*Tharrias*, †*Dastilbe* and *Chanos*.

- †*Knightia* sp.
Specimen number: UMMP Tmp-1008
Position: crown Clupeidae (crown Clupeiformes), Pellonulinae according to (20)
Position in the reference tree: sister to the clade (crown Pellonulinae) comprising *Sierrathrissa leonensis, Pellonula vorax,* their most recent common ancestor and all its descendants
Age / Locality: Eocene / Green River Formation, USA – 55.8-33.9 Ma (20)
Minimum divergence time: †*Knightia* itself is the oldest representative of the total-group Pellonulidae.

- †*Armigatus namourensis* Forey *et al.,* 2003
Specimen number: NHMUK PV P 63151a
Position: stem Clupeiformes according to (21)
Position in the reference tree: sister to the clade (crown Clupeiformes) comprising *Denticeps clupeoides, Pellonula vorax,* their most recent common ancestor and all its descendants
Age / Locality: early to middle Cenomanian / Namoura, Lebanon – 99.7-94.4 Ma (7)
Minimum divergence time: †*Ezkutuberezi carmeni* from the Valanginian, oldest †Ellimichthyiformes (within the clade that †*Armigatus* forms with crown Clupeiformes) – 132.9-139.8 Ma (21)

- †*Ornategulum sardinioides* (Pictet, 1850)
Specimen number: NHMUK PV P 52508
Position: stem Clupeiformes according to (20, 22), possibly as sister to [†*Armigatus* + crown Clupeiformes]
Position in the reference tree: sister to the clade comprising †*Armigatus namourensis*, *Denticeps clupeoides*, their most recent common ancestor and all its descendants
Age / Locality: Cenomanian / Hakel and Namoura, Lebanon (7) – 99.7-94.4 Ma
Minimum divergence time: †*Ezkutuberezi carmeni* from the Valanginian, oldest †Ellimichthyiformes (within the clade that †*Ornategulum* forms with †*Armigatus* and crown Clupeiformes) – 132.9-139.8 Ma (21)

- **†*Plethodus expansus* (Dixon, 1850)**
Specimen number: NHMUK PV P 49895
Position: member of †Tselfatiiformes, which are crown Teleostei, sister to crown Clupeocephala according to (23)
Position in the reference tree: sister to the clade (crown Clupeocephala) comprising *Denticeps clupeoides*, *Oncorhynchus mykiss*, their most recent common ancestor and all its descendants
Age / Locality: Cenomanian-Turonian / English Chalk, UK – 100.5-89.8 Ma (24)
Minimum divergence time: †*Leptolepides* from the Kimmeridgian-Tithonian Solnhofen Limestone is the oldest representative of crown Clupeocephala - 150.94 Ma (15)

- †*Rhacolepis buccalis* Agassiz, 1841
Specimen number: UMMP 101952
Position: within the †Crossognathiformes clade of (25), sister to crown Clupeocephala (that includes Clupeomorpha, Ostariophysi and Euteleostei). According to (23), †Crossognathiformes are sister to [†Tselfatiiformes + crown Clupeocephala]. Sister to Euteleostei (represented by *Salmo salar*) according to (26)
Position in the reference tree: We adopt the phylogenetic position proposed by (25), as it is a recent phylogeny that incorporates many †crossognathiform and crown teleost taxa: sister to the

clade (crown Clupeocephala + †Tselfatiiformes) comprising †*Plethodus expansus*, *Oncorhynchus mykiss*, their most recent common ancestor and all its descendants
Age / Locality: Albian / Santana Formation, Brazil – 113.4-110 Ma (10, 27)
Minimum divergence time: †*Leptolepides sprattiformis* from the Kimmeridgian-Tithonian Solnhofen Limestone is the oldest representative of crown Clupeocephala - 150.94 Ma (15)

- †*Apsopelix anglicus* (Dixon, 1850)
Specimen number: NHMUK PV P 4246
Position: within the †Crossognathiformes clade of (25)
Position in the reference tree: sister to †*Rhacolepis buccalis*
Age / Locality: Cenomanian-Turonian / English Chalk, UK – 100.5-89.8 Ma (24)
Minimum divergence time: †*Bavarichthys incognitus* (13) from the Kimmeridgian-Tithonian Solnhofen Limestone is the oldest representative of the †Crossognathiformes clade of (25) - 150.94 Ma (15)

- †*Phareodus encaustus* Cope, 1871
Specimen number: NHMUK PV P 64636I
Position: stem Osteoglossidae according to (28)
Position in the reference tree: sister to the clade (crown Osteoglossidae) comprising *Osteoglossum bicirrhosum*, *Arapaima gigas*, their most recent common ancestor and all its descendants
Age / Locality: Eocene / Laney Member, Green River Formation, USA - 55.8-33.9 Ma
Minimum divergence time: †*Cretophareodus alberticus* from the Campanian is the oldest representative of the clade formed by †*Phareodus* and crown Osteoglossidae – 83.6-72.1 Ma

- †*Brychaetus muelleri* Woodward, 1901
Specimen number: NHMUK PV OR 28424
Position: sister to †*Phareodus* according to (29)
Position in the reference tree: sister to †*Phareodus encaustus*
Age / Locality: Ypresian / Sheppey, London Clay, UK – 50.5 Ma (24)
Minimum divergence time: †*Brychaetus* itself is the oldest representative of the clade it forms with †*Phareodus*.

- †*Eohiodon falcatus* Grande, 1979
Specimen number: NHMUK PV P 61245
Position: stem Hiodontidae according to (28, 30, 31)
Position in the reference tree: sister to the clade (crown Hiodontidae) comprising *Hiodon alosoides, Hiodon tergisus*, their most recent common ancestor and all its descendants
Age / Locality: Eocene / Green River Formation, USA – 55.8-33.9 Ma
Minimum divergence time: †*Eohiodon* itself is the oldest representative of the clade it forms with *Hiodon*.

Elopomorpha have two alternative topologies in the reference phylogenetic study of (6). Here we chose the hypothesis presented in the Fig. 3 of (6) as it is better resolved for the fossil taxa of our sample.

- †*Hayenchelys germanus* (Hay, 1903)
Specimen number: NHMUK PV P 62726
Position: stem Anguilliformes according to (32)
Position in the reference tree: sister to the clade (crown Anguilliformes) comprising *Diastobranchus capensis* + *Anguilla anguilla*, their most recent common ancestor and all its descendants
Age / Locality: under the †*Mantilliceras mantelli* Ammonite zone, Cenomanian / Hadjula, Lebanon (6) – 98.0 Ma
Minimum divergence time: †*Hayenchelys* itself is the oldest representative of the total-group Anguilliformes.

- †*Istieus grandis* Agassiz, 1842
Specimen number: NHMUK PV P 3886
Position: stem Pterothrissidae according to (6)
Position in the reference tree: sister to *Pterothrissus gissu*
Age / Locality: younger than the †*Scaphites hippocrepis* III Zone but older than the †*Baculites mclearni* Zone (6) / Coesfeld Member of Westphalia, Germany – 81.28-80.67 Ma
Minimum divergence time: †*Istieus* is the oldest representative of the total-group Pterothrissidae.

- †*Lebonichthys gracilis* (Davis, 1887)
Specimen number: NHMUK PV P 49076
Position: stem Albulidae according to (6)
Position in the reference tree: sister to the clade (crown Albulidae) comprising *Albula glossodonta, Albula vulpes*, their most recent common ancestor and all its descendants
Age / Locality: Late Santonian / Sahel Alma, Lebanon – 86.3-83.6 Ma (6, 7)
Minimum divergence time: †*Lebonichthys* itself is the oldest representative of the clade it forms with crown Albulidae.

- †*Brannerion vestitum* Jordan, 1920
Specimen number: NHMUK PV P 60923
Position: sister to [Anguilliformes + Notacanthiformes] according to (6)
Position in the reference tree: †*Brannerion* is found as sister to [Anguilliformes + Notacanthiformes] in (6), but this clade does not exist in the reference phylogeny, unless Albuliformes are also included. We chose the conservative approach to position it as sister to [Anguilliformes + Notacanthiformes + Albuliformes]: the clade comprising *Anguilla anguilla, Albula vulpes*, their most recent common ancestor and all its descendants
Age / Locality: early Albian / Romualdo Member of the Santana Formation, Brazil – 113.4-110 Ma (6)
Minimum divergence time: †*Baugeichthys caeruleus*, earliest representative of the total-group Albuliformes – 134.5-129.4 Ma (1, 6)

- †*Osmeroides* sp. (presumably †*Osmeroides lewesiensis*)
Specimen number: OUMNH K.64151
Position: sister to [Albuliformes + Notacanthiformes + Anguilliformes] according to (6)
Position in the reference tree: sister to the clade comprising †*Brannerion vestitum, Albula vulpes*, their most recent common ancestor and all its descendants [following the proposed position of †*Brannerion*]
Age / Locality: †*Hoplites dentatus* through †*Mortoniceras inflatus* zones of the Albian / Gault Clay Formation, UK – 110.22 Ma
Minimum divergence time: †*Baugeichthys caeruleus*, earliest representative of the total-group Albuliformes – 134.5-129.4 Ma (1, 6)

- †*Flindersichthys denmaedi* Longman, 1932
Specimen number: NHMUK PV P 3886
Position: stem Megalopidae (crown Elopiformes) according to (33)
Position in the reference tree: sister to the clade (crown Megalopidae) comprising *Megalops cyprinoides, Megalops atlanticus*, their most recent common ancestor and all its descendants
Age / Locality: Albian / Stewart Creek, Rolling Downs Formation, Australia – 113.0-100.5 Ma
Minimum divergence time: †*Flindersichthys* itself is the oldest representative of the clade it forms with *Megalops*.

- †*Arratiaelops vectensis* (Woodward, 1890)
Specimen number: NHMUK PV P 42013
Position: stem Megalopidae (crown Elopiformes) according to (33)

Position in the reference tree: sister to the clade comprising †*Flindersichthys denmaedi*, *Megalops cyprinoides*, their most recent common ancestor and all its descendants
Age / Locality: Barremian-Aptian / Bernissart, Belgium – 126.0 Ma
Minimum divergence time: †*Arratiaelops* itself is the earliest representative of the total-group Megalopidae.

- †*Ichthyemidion vidali* Poyato-Ariza, 1995
Specimen number: MNHN.F.MSE356a
Position: stem Elopiformes according to (6)
Position in the reference tree: sister to the clade (crown Elopiformes) comprising *Elops saurus*, *Megalops cyprinoides*, their most recent common ancestor and all its descendants
Age / Locality: Late Berriasian – Early Valanginian / El Montsec, Spain – 131.3-125.9 Ma (6)
Minimum divergence time: †*Ichthyemidion* itself is the oldest representative of the clade it forms with crown Elopiformes.

- †*Anaethalion angustus* (Münster, 1839)
Specimen number: NHMUK PV OR 37926
Position: stem-Elopidae (crown Elopiformes) according to (34), but may be a stem Elopiformes according to (12, 25)
Position in the reference tree: since the position of †*Anaethalion* varies from one phylogenetic analysis to the other, we chose the conservative approach to place it as a stem Elopiformes: sister to the clade comprising †*Ichthyemidion vidali*, *Megalops cyprinoides*, their most recent common ancestor and all its descendants
Age / Locality: †*Neochetoceras rebouletianum* Horizon within the †*Lithacoceras ulmense* Subzone of the †*Hybonoticeras beckeri* Ammonite Zone, Late Kimmeridgian / Eichstätt, Germany – 151.2 Ma (6)
Minimum divergence time: †*Anaethalion* itself is the oldest representative of the total-group Elopiformes, and of crown Elopomorpha.

†Ichthyodectiformes are a clade of stem Teleostei, which position varies from one study to another. Some studies find them as the sister to crown Teleostei (12, 25) while others find some stem Teleostei closer to the crown group than †Ichthyodectiformes (26, 35). We chose to follow (25) since it is a recent phylogenetic analysis including several †ichthyodectiform representatives alongside a comprehensive sample of stem- and crown Teleostei. Other recent large-scale studies either did not include any †ichthyodectiform representative (34, 36) or only one †ichthyodectiform (26). We thus interpret †Ichthyodectiformes as sister to crown Teleostei.

- †*Xiphactinus audax* Leidy, 1870
Specimen number: UMMP 11003
Position: in †Ichthyodectiformes, family †Ichthyodectidae (37)
Position in the reference tree: sister to the clade (crown Teleostei) comprising *Megalops cyprinoides*, *Oncorhynchus mykiss*, their most recent common ancestor and all its descendants
Age / Locality: Turonian-Maastrichtian / USA – 93.9-66 Ma (37)
Minimum divergence time: †*Occithrissops wilsoni* (38) is the oldest representative of †Ichthyodectiformes, and of the clade they form with crown Teleostei – Bathonian, 168.3-166.1 Ma.

- †*Ichthyodectes ctenodon* Cope, 1870
Specimen number: UMMP V56318
Position: in †Ichthyodectiformes, family †Ichthyodectidae (37)
Position in the reference tree: sister to †*Xiphactinus audax*
Age / Locality: Turonian-Campanian / USA – 93.9-72.1 Ma (37)
Minimum divergence time: †*Ichthyodectes* and †*Xiphactinus* themselves are the oldest representatives of the clade (†Ichthyodectidae) they form together.

- †*Eubiodectes libanicus* (Pictet & Humbert, 1866)

Specimen number: NHMUK PV P 62691a
Position: in †Ichthyodectiformes, family †Cladocyclidae (37)
Position in the reference tree: sister to the clade (†Ichthyodectidae) comprising †*Xiphactinus audax*, †*Ichthyodectes ctenodon*, their most recent common ancestor and all its descendants
Age / Locality: Cenomanian / Hakel, Lebanon (7) – 99.7-94.4 Ma
Minimum divergence time: †*Chiromystus mawsoni* is the oldest representative of †Cladocyclidae (and of the clade †*Eubiodectes* forms with †Ichthyodectidae) – Hauterivian-Barremian, 132.9-125 Ma (37).

- †*Thrissops formosus* Agassiz, 1833
Specimen number: NHMUK PV OR 35013
Position: in †Ichthyodectiformes, outside of the clade that includes †Cladocyclidae and †Ichthyodectidae (37)
Position in the reference tree: sister to the clade comprising †*Xiphactinus audax*, †*Eubiodectes libanicus*, their most recent common ancestor and all its descendants
Age / Locality: Kimmeridgian / Eichstätt, Germany – 151.2 Ma (6)
Minimum divergence time: †*Thrissops* itself is the oldest representative of the clade it forms with †Ichthyodectidae and †Cladocyclidae.

- †*Allothrissops regleyi* (Thiollière, 1854)
Specimen number: NHMUK PV P 921
Position: in †Ichthyodectiformes, outside of the clade that includes †*Thrissops*, †Cladocyclidae and †Ichthyodectidae (37)
Position in the reference tree: sister to the clade comprising †*Thrissops formosus*, †*Xiphactinus audax*, their most recent common ancestor and all its descendants
Age / Locality: Kimmeridgian / Eichstätt, Germany – 151.2 Ma (6)
Minimum divergence time: †*Occithrissops wilsoni* (38) is the oldest representative of the clade †*Allothrissops* forms with other †Ichthyodectiformes (37) – Bathonian, 168.3-166.1 Ma.

- †*Pachythrissops laevis* Woodward, 1919
Specimen number: NHMUK PV P 41859
Position: (37) considers the inclusion of †*Pachythrissops* inside †Ichthyodectiformes to be dubious. However, several analyses, including the extensive one of (25) find it to be an †ichthyodectiform, sister to all other members of the clade.
Position in the reference tree: sister to the clade comprising †*Allothrissops regleyi*, †*Xiphactinus audax*, their most recent common ancestor and all its descendants
Age / Locality: Valanginian / Purbeck Group, UK – 139.8-132.9 Ma
Minimum divergence time: †*Occithrissops wilsoni* (38) is the oldest representative of the clade †*Pachythrissops* forms with other †Ichthyodectiformes – Bathonian, 168.3-166.1 Ma (37).

Stem-group teleosts (outside of †Ichthyodectiformes): Several recent phylogenetic studies have tried to resolve the relationships between stem teleost taxa (25, 26, 34, 36, 39). They all recover different topologies for our sampled taxa, but there are several areas of agreement, most notably:
1) a clade including †*Leptolepis coryphaenoides*, †*Tharsis*, †*Ascalabos*, †Ichthyodectiformes (when included) and crown Teleostei;
2) a clade including the above, plus †*Dorsetichthys*, †*Siemensichthys* (and †*Ankylophorus* when included), and †*Eurycormus*;
3) †Pholidophoridae *sensu stricto*, as defined by (34) as sister to this clade;
4) †Aspidorhynchidae and †Pachycormiformes outside of the clade formed by all of the above.
†*Ichthyokentema* is a wildcard taxon and has a different position in every study where it is included.
Since the positions of the different taxa constitutive of these various clades vary from one study to another, we cannot choose which topology is the most likely to reflect reality. In that context, we have chosen to follow the study that has the most comprehensive taxon sample and the best

resolution for each portion of the total-group teleost tree: (25) for the clade described in (1), and (34) for the rest of the tree.

- †*Tharsis dubius* (Blainville, 1818)
Specimen number: NHMUK PV OR 37852b
Position: sister to [†*Ascalabos* + †Varasichthyidae + †Ichthyodectiformes + crown Teleostei] according to (25)
Position in the reference tree: sister to the clade comprising †*Xiphactinus audax*, *Megalops cyprinoides*, their most recent common ancestor and all its descendants
Age / Locality: Kimmeridgian-Tithonian / Solnhofen, Germany –157.3-145 Ma
Minimum divergence time: †*Occithrissops wilsoni* (38) is the oldest representative of the clade †*Ascalabos* forms with crown teleosts (25) – Bathonian, 168.3-166.1 Ma.

- †*Leptolepis coryphaenoides* (Bronn, 1830)
Specimen number: NHMUK PV P 947c
Position: sister to [all of the above, including crown Teleostei] according to (25, 34, 36, 39)
Position in the reference tree: sister to the clade comprising †*Tharsis dubius*, *Megalops cyprinoides*, their most recent common ancestor and all its descendants
Age / Locality: Toarcian / Curcy, France – 182.7-174.1 Ma (26)
Minimum divergence time: †*Leptolepis coryphaenoides* itself is the oldest representative of the clade it forms with crown teleosts.

- †*Leptolepis disjectus* Woodward, 1895
Specimen number: NHMUK PV P 3793a
Position: †*Leptolepis disjectus* is not included in any phylogenetic analysis, therefore we tentatively consider it to be closely related to the congeneric †*L. coryphaenoides*
Position in the reference tree: sister to †*Leptolepis coryphaenoides*
Age / Locality: Bathonian / Thaynton Limestone, UK – 168.3-166.1 Ma
Minimum divergence time: †*Leptolepis coryphaenoides* is the oldest representative of the clade †*Leptolepis* forms with crown teleosts – 182.7-174.1 Ma.

- †*Ichthyokentema purbeckensis* (Davies, 1887)
Specimen number: NHMUK PV P 7807
Position: sister to [†*Leptolepis coryphaenoides* + all of the above, including crown Teleostei], according to (34)
Position in the reference tree: sister to the clade comprising †*Leptolepis coryphaenoides*, *Megalops cyprinoides*, their most recent common ancestor and all its descendants
Age / Locality: Berriasian / Purbeck Group, UK – 145-139.8 Ma
Minimum divergence time: †*Leptolepis coryphaenoides* is the oldest representative of the clade †*Ichthyokentema* forms with crown teleosts – 182.7-174.1 Ma.

- †*Dorsetichthys bechei* (Agassiz, 1837)
Specimen number: OUMNH J.3369
Position: sister to [†*Ichthyokentema* + all of the above, including crown Teleostei] according to (34)
Position in the reference tree: sister to the clade comprising †*Ichthyokentema purbeckensis*, *Megalops cyprinoides*, their most recent common ancestor and all its descendants
Age / Locality: Sinemurian / Lyme Regis, UK – 199.3-190.8 Ma (26, 34)
Minimum divergence time: †*Dorsetichthys* itself is the oldest representative of the clade it forms with crown teleosts.

- †*Siemensichthys macrocephalus* (Agassiz, 1834)
Specimen number: NHMUK PV P 9135
Position: sister to [†*Dorsetichthys* + all of the above, including crown Teleostei] according to (34)
Position in the reference tree: sister to the clade comprising †*Dorsetichthys bechei*, *Megalops cyprinoides*, their most recent common ancestor and all its descendants

Age / Locality: Kimmeridgian-Tithonian / Solnhofen, Germany –157.3-145 Ma
Minimum divergence time: †*Dorsetichthys bechei* is the oldest representative of the clade †*Siemensichthys* forms with crown teleosts – 199.3-190.8 Ma.

- †*Ankylophorus similis* (Woodward, 1895)
Specimen number: NHMUK PV P 1083
Position: sister to †*Siemensichthys* according to (34, 36)
Position in the reference tree: sister to †*Siemensichthys macrocephalus*
Age / Locality: Kimmeridgian-Tithonian / Solnhofen, Germany –157.3-145 Ma
Minimum divergence time: †*Ankylophorus* and †*Siemensichthys* themselves are the oldest representatives of the clade they form together (†Ankylophoridae).

- †*Eurycormus speciosus* Wagner, 1863
Specimen number: MB.f.7016
Position: sister to [†Ankylophoridae + all of the above, including crown Teleostei] according to (34)
Position in the reference tree: sister to the clade comprising †*Siemensichthys macrocephalus*, *Megalops cyprinoides*, their most recent common ancestor and all its descendants
Age / Locality: Kimmeridgian-Tithonian / Solnhofen, Germany –157.3-145 Ma
Minimum divergence time: †*Dorsetichthys bechei* is the oldest representative of the clade †*Eurycormus* forms with crown teleosts – 199.3-190.8 Ma.

- †*Pholidophoropsis caudalis* (Woodward, 1895)
Specimen number: OUMNH J.3363
Position: according to (34), part of †Pholidophoridae *sensu stricto*, a clade of Triassic and Early Jurassic stem Teleostei, represented in the phylogenetic analysis by Triassic genera and not by †*Pholidophoropsis*. The clade is sister to [†*Eurycormus* + all of the above, including crown Teleostei], according to (26, 34)
Position in the reference tree: sister to the clade comprising †*Eurycormus speciosus*, *Megalops cyprinoides*, their most recent common ancestor and all its descendants
Age / Locality: Sinemurian / Lyme Regis, UK – 199.3-190.8 Ma
Minimum divergence time: †*Pholidophoretes salvus* and †*Knerichthys bronni* are the oldest representatives of the †Pholidophoridae *sensu stricto*, and thus of the clade †*Pholidophoropsis* forms with crown teleosts – early Carnian, 237-227 Ma (34).

- †*Pholidophoroides crenulata* Egerton, 1843
Specimen number: NHMUK PV OR 36313
Position: according to (34), part of †Pholidophoridae *sensu stricto*, a clade of Triassic and Early Jurassic stem Teleostei, represented in the phylogenetic analysis by Triassic genera and not by †*Pholidophoroides*. The clade is sister to [†*Eurycormus* + all of the above, including crown Teleostei], according to (26, 34)
Position in the reference tree: sister to †*Pholidophoropsis caudalis*
Age / Locality: Sinemurian / Lyme Regis, UK – 199.3-190.8 Ma
Minimum divergence time: as †*Pholidophoroides* and †*Pholidophoropsis* were never included in a formal phylogenetic analysis, their position within †Pholidophoridae is unknown. Since they are both of the same age and locality, we chose the conservative approach to give their own age as the minimum divergence time for the clade they form together.

- †*Protosphyraena* sp.
Specimen number: NHMUK PV P 9644b
Position: in †Pachycormiformes (40, 41), the latter forming a clade with †Aspidorhynchiformes that is sister to all other total-group Teleostei, according to (26, 34, 36)
Position in the reference tree: sister to the clade comprising †*Prohalecites porroi*, *Megalops cyprinoides*, their most recent common ancestor and all its descendants
Age / Locality: Coniacian-Campanian / Smoky Hill Member, Niobrara Group, USA – 89.8-72.1 Ma

Minimum divergence time: †*Prohalecites porroi* is the oldest representative of the total-group Teleostei – Ladinian-Carnian, 237 Ma (34, 42).

- †*Hypsocormus* sp.
Specimen number: NHMUK PV P 46348b
Position: in †Pachycormiformes, sister to the 'macrocarnivore clade' comprising †*Protosphyraena* (40, 41, 43)
Position in the reference tree: sister to †*Protosphyraena* sp.
Age / Locality: Callovian / Oxford Clay, UK – 166.1-163.6 Ma
Minimum divergence time: †*Hypsocormus* itself is the oldest representative of the clade it forms with †*Protosphyraena* (40, 43).

- †*Rhinconichthys taylori* Friedman *et al.*, 2010
Specimen number: NHMUK PV OR 33219
Position: in †Pachycormiformes, sister to the clade comprising †*Hypsocormus* and †*Protosphyraena* (40, 41, 43)
Position in the reference tree: sister to the clade comprising †*Protosphyraena* sp., †*Hypsocormus* sp., their most recent common ancestor and all its descendants
Age / Locality: Lower Chalk, Cenomanian / Burnham, UK – 100.5-93.3 Ma (41)
Minimum divergence time: †*Pachycormus*, †*Euthynotus* and other taxa are the oldest representatives of the clade †*Rhinconichthys* forms with †*Protosphyraena* and †*Hypsocormus* (40, 43) – late Toarcian, 182.7-174.1 Ma.

- †*Pachycormus macropterus* (Blainville, 1818)
Specimen number: MNHN.F.STC103 (as. †*P. curtus*)
Position: in †Pachycormiformes, sister to the 'filter-feeding clade' comprising †*Rhinconichthys* (40, 41, 43). †*Pachycormus curtus* is considered a junior synonym of †*P. macropterus* by (43)
Position in the reference tree: sister to †*Rhinconichthys taylori*
Age / Locality: late Toarcian / Curcy, France – 182.7-174.1 Ma
Minimum divergence time: †*Pachycormus* itself is the oldest representative of the clade it forms with †*Rhinconichthys* (40, 43).

- †*Euthynotus incognitus* (Blainville, 1818)
Specimen number: NHMUK PV P 2044
Position: in †Pachycormiformes, sister to all other members of the clade (40, 41, 43)
Position in the reference tree: sister to the clade comprising †*Protosphyraena* sp., †*Pachycormus macropterus*, their most recent common ancestor and all its descendants
Age / Locality: Toarcian / *Posidonia* shale, Holzmaden, Germany – 182.7-174.1 Ma
Minimum divergence time: †*Euthynotus* itself is the oldest representative of †Pachycormiformes (40, 43).

- †*Vinctifer comptoni* (Agassiz, 1841)
Specimen number: UMMP 101950
Position: in †Aspidorhynchiformes, themselves sister to †Pachycormiformes according to (26, 34, 36)
Position in the reference tree: sister to the clade (†Pachycormiformes) comprising †*Euthynotus incognitus*, †*Pachycormus macropterus*, their most recent common ancestor and all its descendants
Age / Locality: early Albian / Romualdo Member of the Santana Formation, Brazil – 113.4-110 Ma (44)
Minimum divergence time: †*Euthynotus incognitus* is the oldest representative of the [†Pachycormiformes + †Aspidorhynchiformes] clade (26, 40) – Toarcian, 182.7-174.1 Ma.

- †*Belonostomus* sp.
Specimen number: NHMUK PV P 4029
Position: in †Aspidorhynchiformes, sister to †*Vinctifer* according to (44)

Position in the reference tree: sister to †*Vinctifer comptoni*
Age / Locality: early to middle Cenomanian / Namoura, Lebanon – 99.7-94.4 Ma (7, 44)
Minimum divergence time: †*Belonostomus tenuirostris* and †*B. dorsetensis* are the oldest representatives of †*Belonostomus* – Kimmeridgian, 157.3-152.1 Ma (44).

- †*Belonostomus muensteri* (Agassiz, 1834)
Specimen number: NHMUK PV OR 37796
Position: in †*Belonostomus* according to (44)
Position in the reference tree: sister to †*Belonostomus* sp.
Age / Locality: Tithonian / Solnhofen Limestone, Germany – 152.1-145 Ma (44)
Minimum divergence time: †*Belonostomus tenuirostris* and †*B. dorsetensis* are the oldest representatives of †*Belonostomus* – Kimmeridgian, 157.3-152.1 Ma (44).

- †*Aspidorhynchus fisheri* Egerton, 1854
Specimen number: NHMUK PV P 17317
Position: in †Aspidorhynchiformes, sister to [†*Belonostomus* + †*Vinctifer*] according to (44)
Position in the reference tree: sister to the clade comprising †*Vinctifer comptoni*, †*Belonostomus* sp., their most recent common ancestor and all its descendants
Age / Locality: Berriasian / Purbeck Group, UK – 145-139.8 Ma
Minimum divergence time: †*Aspidorhynchus crassus* is the oldest representative of †Aspidorhynchiformes – Bathonian, 168.3-166.1 Ma (44).

- †*Aspidorhynchus acutirostris* (Blainville, 1818)
Specimen number: NHMUK PV P 97
Position: in †*Aspidorhynchus* according to (44)
Position in the reference tree: sister to †*Aspidorhynchus fisheri*
Age / Locality: Kimmeridgian / Kimmeridge Clay, UK– 157.3-152.1 Ma
Minimum divergence time: †*Aspidorhynchus crassus* is the oldest representative of †Aspidorhynchiformes – Bathonian, 168.3-166.1 Ma (44).

- †*Semionotus elegans* Newberry, 1888
Specimen number: UMMP 13664
Position: stem Gynglimodi according to (26)
Position in the reference tree: sister to the clade (crown Gynglimodi) comprising *Atractosteus tropicus*, *Lepisosteus osseus*, their most recent common ancestor and all its descendants
Age / Locality: Hettangian-Sinemurian / Newark Supergroup, USA – 201.3-190.8 Ma (26, 45)
Minimum divergence time: †*Semionotus bergeri* is the oldest representative of the clade †*S. elegans* forms with crown Gynglimodi – Carnian, 237-227 Ma (26).

- †*Heterolepidotus dorsalis* Kner, 1866
Specimen number: NHMUK PV P 10290
Position: stem Halecomorphi, potentially close to †*Ophiopsis* according to (46) but never included in a phylogenetic analysis
Position in the reference tree: sister to *Amia calva* (crown Halecomorphi)
Age / Locality: Rhaetian / Hallein, Germany – 208.5-201.3 Ma
Minimum divergence time: †*Heterolepidotus* itself is the oldest representative of the clade it forms with crown Halecomorphi.

- †*Eoeugnathus megalepis* Brough, 1939
Specimen number: PIMUZ T344
Position: stem Halecomorphi, close to †*Panxianichthys* and thus outside of the clade formed by †*Ophiopsis* (and thus †*Heterolepidotus*) and *Amia* according to (26, 47)
Position in the reference tree: sister to the clade comprising †*Heterolepidotus dorsalis*, *Amia calva*, their most recent common ancestor and all its descendants
Age / Locality: Ladinian / Monte San Giorgio, Switzerland – 242-237 Ma

Minimum divergence time: †*Panxianichthys imparilis* is the oldest representative of the clade †*Eoeugnathus* forms with crown Halecomorphi – Anisian, 247.2-242 Ma.

- **†*Dapedium* cf. *politum* Leach, 1822**
Specimen number: OUMNH J.3323
Position: in †Dapediiformes, stem Holostei according to (26, 48)
Position in the reference tree: sister to the clade (crown Holostei) comprising *Lepisosteus osseus*, *Amia calva*, their most recent common ancestor and all its descendants
Age / Locality: Sinemurian / Lyme Regis, UK – 199.3-190.8 Ma (49)
Minimum divergence time: †*Watsonulus eugnathoides* is the oldest representative of crown Holostei, and of the clade †*Dapedium* forms with them – Induan-Olenekian, 251.9-247.2 Ma (26, 50).

- †*Perleidus* sp.
Specimen number: NHMUK PV P 26456
Position: stem Neopterygii, according to (51, 52)
Position in the reference tree: sister to the clade (crown Neopterygii) comprising *Amia calva*, *Megalops cyprinoides*, their most recent common ancestor and all its descendants
Age / Locality: *Proptychites* beds, Induan / Stensiö Plateaus, Greenland – 251.9-251.2 Ma
Minimum divergence time: †*Perleidus* itself is the oldest representative of the clade it forms with crown Neopterygii (53).

- †*Pholidopleurus typus* Bronn, 1858
Specimen number: NHMUK PV P 19314
Position: in †Pholidopleuridae, stem Neopterygii, outside of [†*Perleidus* + crown Neopterygii] according to (51, 52)
Position in the reference tree: sister to the clade comprising †*Perleidus* sp., *Megalops cyprinoides*, their most recent common ancestor and all its descendants
Age / Locality: Anisian-Ladinian / Besano, Italy – 247.2-237 Ma
Minimum divergence time: †*Perleidus* is the oldest representative of the clade †*Pholidopleurus* forms with crown Neopterygii – 251.9-251.2 Ma.

- †*Proscinetes elegans* (Agassiz, 1833)
Specimen number: NHMUK PV P 1626
Position: in †Pycnodontiformes, that are stem Neopterygii according to (48). †Pycnodontiformes, †*Pholidopleurus* and †*Perleidus* have never been included in the same phylogenetic analysis, so we choose the conservative approach and place †*Proscinetes* outside of the clade [†*Perleidus* + †*Pholidopleurus* + crown Neopterygii]
Position in the reference tree: sister to the clade comprising †*Pholidopleurus typus*, *Megalops cyprinoides*, their most recent common ancestor and all its descendants
Age / Locality: lower Tithonian / Solnhofen, Germany – 152.1-145 Ma (54)
Minimum divergence time: †*Perleidus* is the oldest representative of the clade †*Proscinetes* forms with crown Neopterygii – 251.9-251.2 Ma.

- †*Birgeria stensioei* Aldinger, 1931
Specimen number: PIMUZ T2188
Position: traditionally viewed as a stem Chondrostei (50), †*Birgeria* is a stem Actinopteri according to (55)
Position in the reference tree: sister to the clade (crown Actinopteri) comprising *Acipenser transmontanus*, *Megalops cyprinoides*, their most recent common ancestor and all its descendants
Age / Locality: Anisian-Ladinian / Besano, Italy – 247.2-237 Ma (56)
Minimum divergence time: †*Discoserra pectinodon* is the oldest representative of the total-group Neopterygii, and crown Actinopteri (50, 55) – Bashkirian, 323.2-315.2 Ma.

I.3. Quality control criteria and specimens excluded from the analysis

We performed an initial quality-control evaluation of our scan data based on a list of three objective criteria. Specimens that did not pass any one of these criteria were not included in our analysis of evolution of osteocyte volumes and inferred genome size through time:
- (1) It was possible to confidently identify osteocyte lacunae in the PPC-SRμCT tomograms. Specimens lacking osteocytes, or in which osteocytes could not be confidently identified were not included in the analysis;
- (2) The osteocyte lacunae were well-preserved or well-defined enough in the PPC-SRμCT tomograms to guarantee that their volumes would be accurately measured. Poor definition or preservation could result from taphonomic factors (e.g. infilling of the lacunae by mineral-rich fluids) or issues with the scans themselves causing low contrast between fossil bone and its lacunae;
- (3) Sufficiently large numbers of osteocyte lacunae were present in the scan (count > ~50) to provide quantitative confidence in estimates of their average volumes. Specimens that had fewer osteocyte lacunae, even if they were well-defined, were excluded from the analysis.

- †*Oncorhynchus lacustris* (Cope, 1870)
Specimen numbers: UMMP 47839, UMMP 52619, UMMP 21756.
Position: in Salmonidae, close to *Oncorhynchus mykiss* according to (2, 3)
Age / Locality: Miocene / Chalk Hills Formation, USA – 9.8-4.8 Ma (2, 4)
Failed criterion 2.

- †*Paleolox larsoni* Kimmel, 1975
Specimen number: UMMP 50352.
Failed criterion 2.

- †*Lycoptera middendorffi* Müller, 1848
Specimen number: NHMUK PV P 6728.
Position: stem Osteoglossomorpha according to (28)
Age / Locality: Early Cretaceous / Mt Uksuk, Mongolia – 136.4-125.5 Ma
Failed criterion 2.

- †*Anaethalion angustus* (Münster, 1839)
Specimen number: NHMUK PV P 3575.
Failed criteria 2 and 3.

- †*Cladocyclus gardneri* Agassiz, 1841
Specimen number: UMMP 117484.
Position: in †Ichthyodectiformes, family †Cladocyclidae (37)
Age / Locality: Aptian-Albian / Crato and Santana Formations, Brazil – 123-110 Ma (37)
Failed criteria 2 and 3.

- †*Ascalabos voithii* Münster, 1839
Specimen number: NHMUK PV P 3673a.
Position: sister to [†Ichthyodectiformes + crown Teleostei] according to (25)
Age / Locality: Kimmeridgian / Kelheim, Germany – 157.3-152.1 Ma
Failed criteria 2 and 3.

- **†*Lombardichthys gervasuttii* (Zambelli, 1980)**
Specimen number: MCSNB 6662.
Position: part of †Pholidophoridae *sensu stricto* (36)
Age / Locality: Norian / Ponte Giurino, Italy – 210 Ma (34, 36)
Failed criterion 1.

- †*Pholidorhynchodon malzannii* Zambelli, 1980

Specimen number: MCSNB 11015.
Position: part of †Pholidophoridae *sensu stricto* (34, 36)
Age / Locality: Norian / Cene, Italy – 210 Ma (34, 36)
Failed criterion 1.

- †*Parapholidophorus nybelini* Zambelli, 1975
Specimen number: MCSNB 6530c.
Position: part of †Pholidophoridae *sensu stricto* (34, 36)
Age / Locality: Norian / Cene, Italy – 210 Ma (34, 36)
Failed criterion 1.

- †*Pholidoctenus serianus* Zambelli, 1977
Specimen number: MCSNB 4827.
Position: part of †Pholidophoridae *sensu stricto* (34, 36)
Age / Locality: Norian / Cene, Italy – 210 Ma (34, 36)
Failed criterion 1.

- †*Prohalecites porroi* (Bellotti, 1857)
Specimen number: NHMUK PV P 19471.
Position: sister to [†Pholidophoridae *sensu stricto* + all other total-group Teleostei] according to (34, 36)
Age / Locality: Ladinian-Carnian boundary / Perledo, Italy – 237 Ma (42)
Failed criteria 2 and 3.

- †*Pachycormus macropterus* (Blainville, 1818)
Specimen number: NHMUK PV P 32433.
Failed criterion 2.

- †*Aspidorhynchus acutirostris* (Blainville, 1818)
Specimen number: NHMUK PV P 56466.
Failed criterion 2.

- †*Cheirolepis canadensis* Whiteaves, 1881
Specimen number: UMMP 3453.
Position: stem Actinopterygii according to (48, 55, 57, 58)
Age / Locality: Escuminac Formation, Frasnian / Miguasha, Canada – 382.7-372.2 Ma (59)
Failed criterion 2.

II. Comments on Triassic stem-group teleosts

Stem-group teleosts are known since the Middle Triassic, the oldest ones being the pholidophorids †*Malingichthys nimaiguensis* and †*M. wanfenglinensis* from the late Ladinian (239-238 Ma) of southern China (60). These species are slightly older than †*Prohalecites porroi* from the latest Ladinian (237 Ma) of the Perledo-Varenna Formation (Grigna Mountains, Italy) and Kalkschieferzone (Meride Limestone) of Monte San Giorgio (42). In order to reflect as accurately as possible the temporal distribution of total-group teleosts, we included five Triassic stem-group teleosts in our sample: †*Prohalecites porroi* (NHMUK PV P 19471), as well as the Norian †*Lombardichthys gervasuttii* (MCSNB 6662), †*Pholidorhynchodon malzannii* (MCSNB 11015), †*Parapholidophorus nybelini* (MCSNB 6530c) and †*Pholidoctenus serianus* (MCSNB 4827) from Northern Italy (34, 36). All of these five Triassic taxa were represented by one sample from the dentary (lower jaw), and SRμCT-scanned at the Diamond Light Source I13-2 beamline, U.K. They were no issues with the SRμCT data acquisition itself, however, none of the four Norian specimens apparently preserved osteocyte lacunae. The apparent absence of preserved osteocyte lacunae may be related to the presence of abundant synsedimentary pyrite in fossils from these localities (61), which may have affected the skeletal tissue obliterating any evidence of cellular structure, but additional data on the taphonomy of the localities would be needed to substantiate this hypothesis. There is no reason to believe that osteocytes were absent in these taxa (i.e. anosteocytic bone (62, 63)), because other histological structures (e.g., growth lines, lines of reversal) were not visible either. Conversely, osteocyte lacunae have been detected and segmented in †*Prohalecites porroi*. However, only very few of them were preserved in the examined sample for this species and their preservation was poor, limiting their statistical power and potentially introducing a bias. For this reason, and because of the strong influence of this taxon on the results, we chose not to include it in the analyses. Due to the impossibility to obtain information from Triassic stem-group teleosts, the oldest total-group teleosts present in our sample are the Early Jurassic (Sinemurian) †*Pholidophoroides crenulata* and †*Pholidophoropsis caudalis* from Lyme Regis, U.K. Future investigations should aim to include Triassic stem-teleosts in order to more precisely define the age of the teleost WGD. Additional taxa not sampled in this study which could be targeted are †*Annaichthys pontegiurinensis*, †*Eopholidophorus forojuliensis*, †*Jiangilichthys* sp., †*Knerichthys bronni*, †*Parapholidophorus caffi*, †*Pholidophoretes salvus*, †*Pholidophorus gervasuttii*, †*Pholidophorus latiusculus* and †*Zambellichthys bergamensis* (34, 64). In addition, a few enigmatic Middle Triassic neopterygians may represent the earliest stem-group teleosts, including the middle Anisian (about 242 Ma) †*Marcopoloichthys ani* from the Upper Member of the Guangling Formation, Yunnan, South China (65). This taxon is characterized by a unique combination of features, including an apparently mobile premaxilla, a dorso-ventrally symmetrical caudal fin with a reduced number of hypurals, and an extreme reduction of the cover of ganoid scales (65, 66). A reevaluation of the phylogenetic position of this taxon would be desirable to address key questions about the earliest stages of teleost evolution, the origin of teleost morphological innovations and of their WGD.

III. Synchrotron beamline setups

III.1. DLS I13-2 Diamond-Manchester Imaging beamline setup

The X-ray beam was generated by a 2 m long in vacuum undulator (gap 5 mm), filtered with pyrolytic graphite (1340 μm), aluminium (2100 μm) and molybdenum (84 μm). Additionally, a rhodium mirror was used to cut high energies. It resulted in a weighted mean detected energy of 21.39 keV. Radiographs were recorded using an indirect detector comprising a 34 μm GGG scintillator, a 10x microscope lens, a 2x eyepiece and a PCO.edge 5.5 sCMOS camera (PCO AG, Kelheim, Germany). The effective recorded pixel size for this system was 0.357 μm. Based on the pixel size and the detected energy, the sample-detector propagation distance was set to 17 mm. The acquisition consisted of 2500 projections recorded over a 180° rotation of the sample, with an exposure time of 0.5 s per projection. Additionally, 20 flatfield images (sample out

of the beam) were recorded before and after the scan as well as 20 dark images before the beginning of the scan (X-ray beam off to record the noise of the camera). Tomographic reconstruction was performed using the Savu processing pipeline (67) and the I13 analysis Python package. The workflow consisted of a dezinger correction (i.e. removing the scattering spikes), an optical distortion correction, ring removal on sinogram, single distance phase retrieval using the Paganin filter (68), tomographic reconstruction using TomoPy (69), and a conversion of the 32-bits HDF5 volume as a 16-bits tiff stack.

III.2. ESRF ID19 beamline setup

The ID19 beamline could be tuned for a much broader range of energies and the setup was regularly changed to adjust to the sample (see Supplementary Data). The X-ray beam was generated either by a wiggler or a single harmonic undulator, depending on the required energy. Filters were also adjusted depending on the energy. Beryllium X-ray lenses were used to focus the beam and increase flux on the sample (number of lenses adjusted with energy). Finally, we used a 1 mm graphite rotating disk as a decoherer and reduce potential ring artefact (70). Radiographs were recorded using an indirect detector comprising a scintillator (10 µm GGG or 25 µm LuAG), a 10x microscope lens and a PCO.edge camera (5.5 or 4.2 gold). The effective pixel size for this system was ca. 0.7 µm (as small variations were induced by changing the propagation distance). Based on the pixel size and the detected energy, the sample-detector propagation distance was adjusted, ranging from 20 to 220 mm. The acquisition consisted of 2999 projections recorded over a 360° rotation of the sample. Exposure time was ranging from 0.03 to 0.2 seconds, as transmitted signal was getting lower as the energy increased. Additionally, 21 flatfield images (sampled out of the beam) were recorded before and after the scan as well as 20 dark images before the beginning of the scan (X-ray beam off to record the noise of the camera). Tomographic reconstruction was performed using PyHST2 (71). The workflow consisted of a tomographic reconstruction using the single distance phase retrieval approach of PyHST2, followed by a conversion of the 32-bits EDF stack as a 16-bits tiff stack. Additional processing included ring correction (72).

III.3. Note on the resolution

Outside of the higher energies available at the ESRF ID19 beamline, the second main difference between both beamlines was the magnification setups, generating data with a recorded voxel size of 0.357 µm at the I13-2 beamline and near 0.7 µm at the ID19 beamline. It is important to note that these values indicate the magnification only and not the resolution, i.e. the smallest feature observable in the resulting tomographic data. Several parameters will influence the resolution, including notably the brilliance and spatial coherence of the incoming X-ray beam, the thickness and composition of the scintillator, the optical lenses and the digital camera. As the aim of this project is to measure osteocyte volumes, the variation in magnification and possibly in resolution could affect: 1) the smallest osteocyte detected; 2) the volume of osteocytes by adding or removing voxels at the periphery of the volume. The smallest osteocytes measured have a volume of ca. 70 µm3; such a volume would be defined by ca. 1500 voxels and 195 voxels for voxel sizes of 0.357 µm and 0.7 µm respectively. The variation in voxel size hence could not influence the detection of the smallest osteocytes in our dataset.

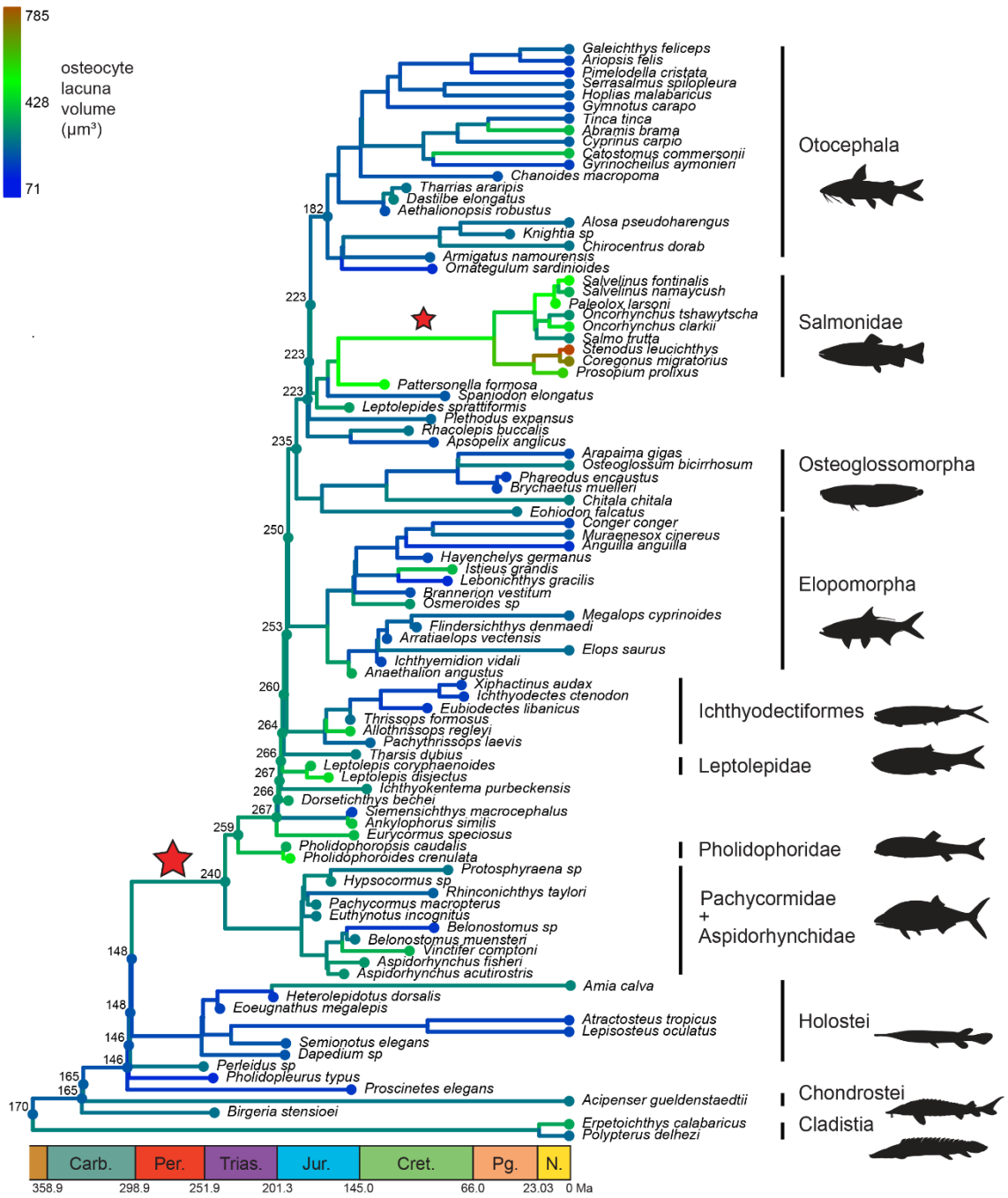

Figure S1. Evolution of osteocyte lacuna volume in fossil and modern teleosts revealed by synchrotron microtomography. Timescaled composite phylogeny of actinopterygians with mapped cell-size volumes for fossil and modern lineages. This version includes terminal taxon names.

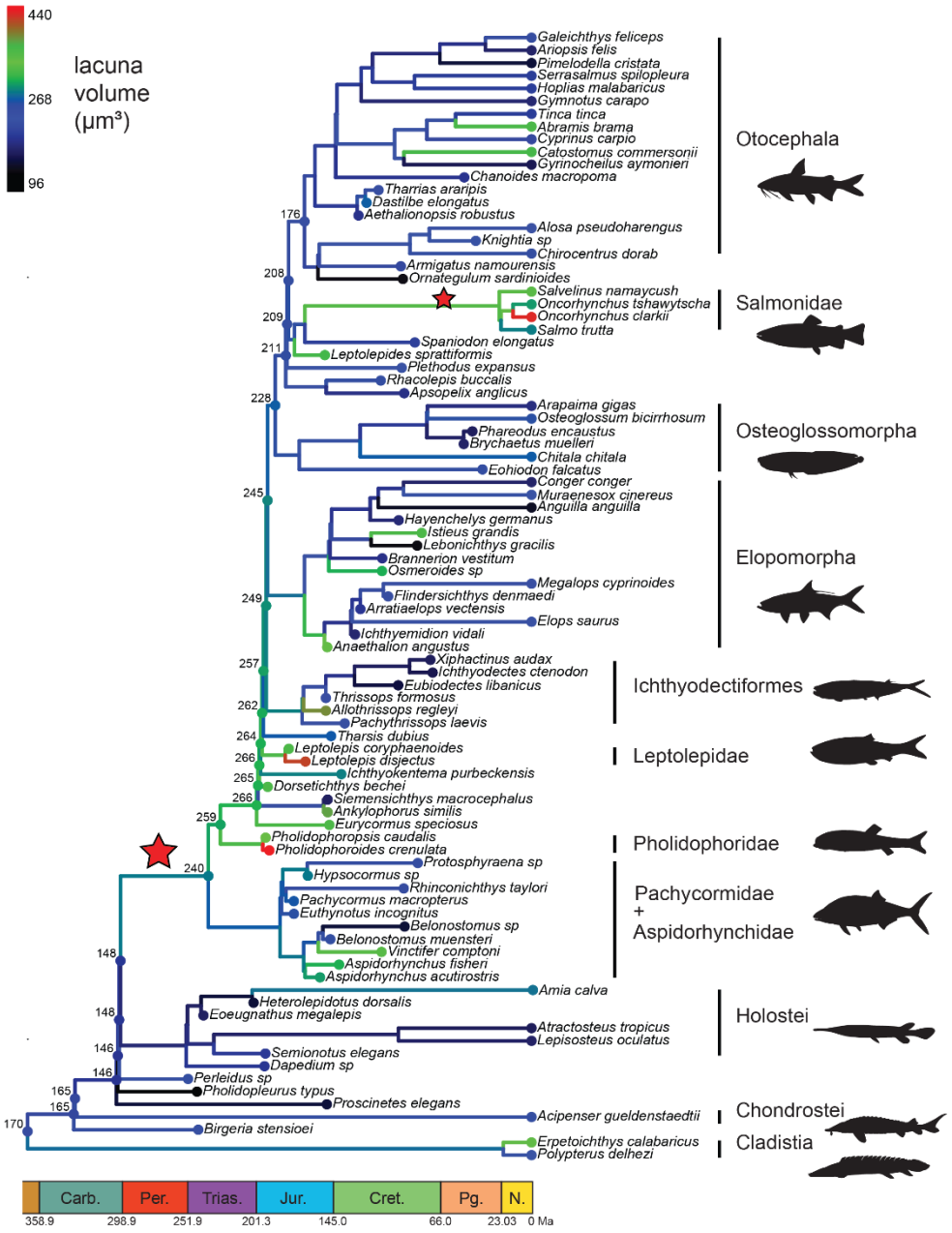

Figure S2. Evolution of osteocyte lacuna volume in fossil and modern teleosts revealed by synchrotron microtomography. Alternative version of Fig. 1 where *Salvelinus fontinalis*, *Coregonus migratorius*, *Stenodus leucichthys*, *Prosopium prolixus*, *Paleolox larsoni*, and *Pattersonella formosa* were omitted due to their very large osteocyte lacuna volumes. Therefore, the color scale distinguishes better the variation in volume of most of the taxon sample. This scale is different to that of Figs. 1-2.

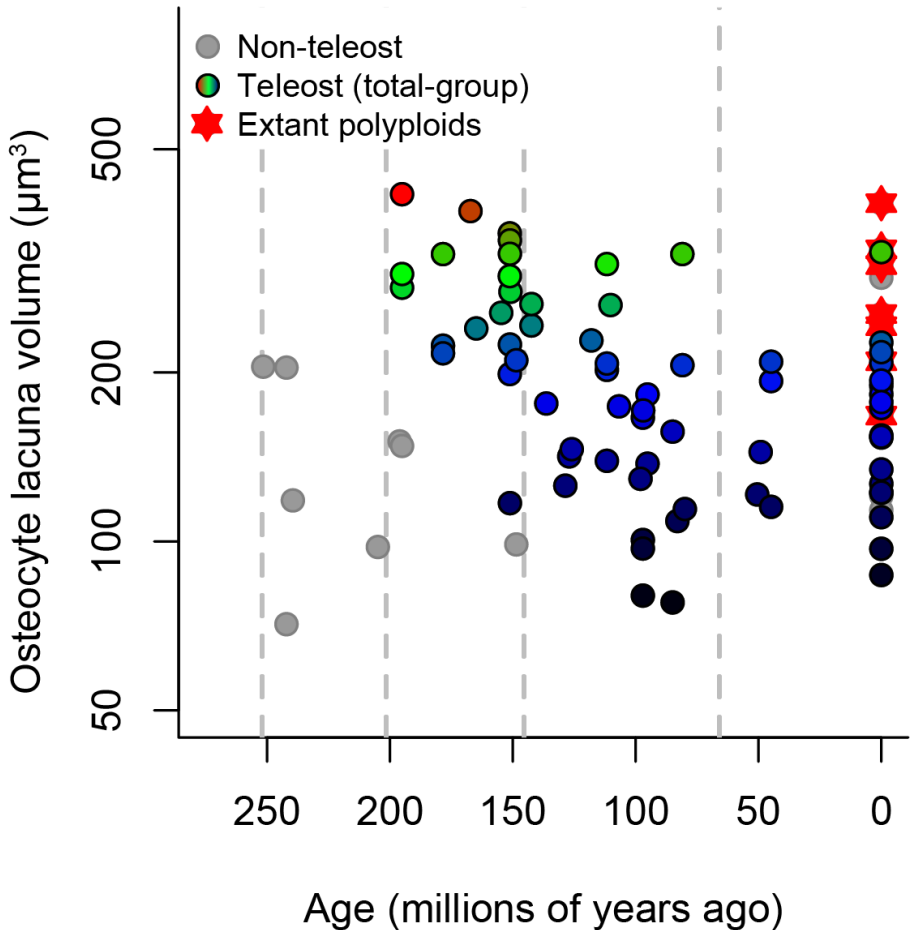

Figure S3. Evolution of osteocyte lacuna volume in fossil and modern teleosts revealed by synchrotron microtomography, plotted against time. Alternative version of Fig. 2, omitting the same taxa and using the same color scale as Fig. S2.

Dataset S1 (separate file). Full list of specimens used in the study, with their age ranges, the specifier taxa for their sister clades, and minimum divergence times from those sister clades based on fossil occurrences.

Dataset S2 (separate file). Full list of specimens for which PPC-SRµCT data were obtained, with the corresponding detailed experimental setups.

Dataset S3 (separate file). Tree file used in our analysis, obtained from stitching fossil taxa to the reference tree (1).

Dataset S4 (separate file). Full list of specimens, with the corresponding median osteocyte volumes using the minimum and maximum realistic grey value thresholds. We only used the "max" values for the analyses.

SI References

1. D. L. Rabosky, *et al.*, An inverse latitudinal gradient in speciation rate for marine fishes. *Nature* **559**, 392–395 (2018).
2. R. F. Stearley, G. R. Smith, Fishes of the Mio-Pliocene Western Snake River plain and vicinity I. Salmonid fishes from Mio-Pliocene lake sediments in the Western Snake River plain and the Great Basin. *Misc. Publ. Museum Zool. Univ. Michigan* **204**, 1–43 (2016).
3. R. F. Stearley, G. R. Smith, Phylogeny of the Pacific trouts and salmons (*Oncorhynchus*) and genera of the family Salmonidae. *Trans. Am. Fish. Soc.* **122**, 1–33 (1993).
4. M. A. Alexandrou, B. A. Swartz, N. J. Matzke, T. H. Oakley, Genome duplication and multiple evolutionary origins of complex migratory behavior in Salmonidae. *Mol. Phylogenet. Evol.* **69**, 514–523 (2013).
5. L. Taverne, A. Filleul, Osteology and relationships of the genus *Spaniodon* (Teleostei, Salmoniformes) from the Santonian (Upper Cretaceous) of Lebanon. *Palaeontology* **46**, 927–944 (2003).
6. A. Dornburg, M. Friedman, T. J. Near, Phylogenetic analysis of molecular and morphological data highlights uncertainty in the relationships of fossil and living species of Elopomorpha (Actinopterygii: Teleostei). *Mol. Phylogenet. Evol.* **89**, 205–218 (2015).
7. P. L. Forey, L. Yi, C. Patterson, C. E. Davies, Fossil fishes from the Cenomanian (Upper Cretaceous) of Namoura, Lebanon. *J. Syst. Palaeontol.* **1**, 227–330 (2003).
8. L. Taverne, Sur *Pattersonella formosa* (Traquair, 1911) et *Nybelinoides brevis* (Traquair, 1911), téléostéens salmoniformes argentinoides du Wealdien inférieur de Bernissart, Belgique, précédemment attribués au genre *Leptolepis* Agassiz, 1832. *Bull. l'Institut R. Sci. Nat. Belgique, Sci. la Terre* **54**, 1–27 (1982).
9. S. Olive, L. Taverne, L. Cavin, U. Deesri, Systematic revision of the Cretaceous actinopterygian fauna from Bernissart, Belgium. *Res. Knowl.* **3**, 43–46 (2017).
10. T. J. Near, A. Dornburg, M. Friedman, Phylogenetic relationships and timing of diversification in gonorynchiform fishes inferred using nuclear gene DNA sequences (Teleostei: Ostariophysi). *Mol. Phylogenet. Evol.* **80**, 297–307 (2014).
11. G. Arratia, Basal teleosts and teleostean phylogeny. *Palaeo Ichthyol.* **7**, 5–168 (1997).
12. G. Arratia, Remarkable teleostean fishes from the Late Jurassic of southern Germany and their phylogenetic relationships. *Mitteilungen aus dem Museum für Naturkd. zu Berlin, Geowissenschaftliche R.* **3**, 137–179 (2000).
13. G. Arratia, H. Tischlinger, The first record of Late Jurassic crossognathiform fishes from Europe and their phylogenetic importance for teleostean phylogeny. *Foss. Rec.* **13**, 317–341 (2010).
14. L. B. Bean, G. Arratia, Anatomical revision of the Australian teleosts *Cavenderichthys talbragarensis* and *Waldmanichthys koonwarri* impacting on previous phylogenetic interpretations of teleostean relationships. *Alcheringa An Australas. J. Palaeontol.* (2019) https:/doi.org/10.1080/03115518.2019.1666921.
15. M. J. Benton, *et al.*, Constraints on the timescale of animal evolutionary history. *Palaeontol. Electron.* **18.1.1FC**, 1–106 (2015).
16. C. Patterson, *Chanoides*, a marine Eocene otophysan fish (Teleostei: Ostariophysi). *J. Vertebr. Paleontol.* **4**, 430–456 (1984).
17. D. Mayrinck, P. M. Brito, O. Otero, Review of the osteology of the fossil fish formerly attributed to the genus †*Chanoides* and implications for the definition of otophysan bony characters. *J. Syst. Palaeontol.* **13**, 397–420 (2015).
18. D. Mayrinck, "Relações Filogenéticas dos Otophysi (Actinopterygii, Teleostei), com ênfase em Characiformes, incluindo as formas fósseis," Université de Poitiers - Universidade do Estado do Rio de Janeiro. (2010).
19. L. Taverne, Ostéologie et position systématique d'*Aethalionopsis robustus* (Pisces, Teleostei) du Crétacé inférieur de Bernissart (Belgique) et considérations sur les affinités des Gonorhynchiformes. *Bull. la Cl. des Sci. Académie R. Belgique* **5**, 958–982 (1981).
20. L. Grande, Recent and fossil clupeomorph fishes with materials for revision of the subgroups of clupeoids. *Bull. Am. Museum Nat. Hist.* **181**, 231–372 (1985).
21. J. Alvarado-Ortega, E. Ovalles-Damián, G. Arratia, "A review of the interrelationships of

the order Ellimmichthyiformes (Teleostei: Clupeomorpha)" in *Mesozoic Fishes 4 - Homology and Phylogeny*, G. Arratia, H.-P. Schultze, M. V. H. Wilson, Eds. (Verlag Dr. Friedriech Pfeil, 2008), pp. 257–278.
22. P. L. Forey, A primitive clupeomorph fish from the middle Cenomanian of Hakel, Lebanon. *Can. J. Earth Sci.* **10**, 1302–1318 (1973).
23. L. Taverne, *Tselfatia formosa*, téléostéen marin du Crétacé (Pisces, Actinopterygii), et la position systématique des Tselfatiiformes ou Bananogmiiformes. *Geodiversitas* **22**, 5–22 (2000).
24. M. Friedman, H. T. Beckett, R. A. Close, Z. Johanson, The English Chalk and London Clay: two remarkable British bony fish *Lagerstätten*. *Geol. Soc. London, Spec. Publ.* **430**, 165–200 (2016).
25. E. Sferco, A. López-Arbarello, A. M. Báez, Phylogenetic relationships of †*Luisiella feruglioi* (Bordas) and the recognition of a new clade of freshwater teleosts from the Jurassic of Gondwana. *BMC Evol. Biol.* **15**, 268 (2015).
26. A. López-Arbarello, E. Sferco, Neopterygian phylogeny: the merger assay. *R. Soc. Open Sci.* **5**, 172337 (2018).
27. P. L. Forey, The osteology of *Notelops* Woodward, *Rhacolepis* Agassiz and *Pachyrhizodus* Dixon (Pisces: Teleostei). *Bull. Br. Museum (Natural Hist. Geol.* **28**, 123–204 (1977).
28. A. M. Murray, D. K. Zelenitsky, D. B. Brinkman, A. G. Neuman, Two new Palaeocene osteoglossomorphs from Canada, with a reassessment of the relationships of the genus †*Joffrichthys*, and analysis of diversity from articulated versus microfossil material. *Zool. J. Linn. Soc.* **183**, 907–944 (2018).
29. J. Zhang, Phylogeny of Osteoglossomorpha. *Vertebr. Palasiat.* **44**, 43–59 (2006).
30. L. Grande, *Eohiodon falcatus*, a new species of hiodontid (Pisces) from the late Early Eocene Green River Formation of Wyoming. *J. Paleontol.* **53**, 103–111 (1979).
31. E. J. Hilton, Comparative osteology and phylogenetic systematics of fossil and living bony-tongue fishes (Actinopterygii, Teleostei, Osteoglossomorpha). *Zool. J. Linn. Soc.* **137**, 1–100 (2003).
32. A. Belouze, M. Gayet, C. Atallah, Les premiers Anguilliformes : II. Paraphylie du genre *Urenchelys* Woodward, 1900 et relations phylogénétiques. *Geobios* **36**, 351–378 (2003).
33. L. Taverne, Ostéologie et position systématique d'*Arratiaelops vectensis* gen. nov., téléostéen élopiforme du Wealdien (Crétacé inférieur) d'Angleterre et de Belgique. *Bull. l'Institut R. Sci. Nat. Belgique, Sci. la Terre* **39**, 77–96 (1999).
34. G. Arratia, Morphology, taxonomy, and phylogeny of Triassic pholidophorid fishes (Actinopterygii, Teleostei). *J. Vertebr. Paleontol.* **33**, 1–138 (2013).
35. C. Patterson, D. E. Rosen, Review of ichthyodectiform and other Mesozoic teleost fishes and the theory and practice of classifying fossils. *Bull. Am. Museum Nat. Hist.* **158**, 81–172 (1977).
36. G. Arratia, New Triassic teleosts (Actinopterygii, Teleosteomorpha) from northern Italy and their phylogenetic relationships among the most basal teleosts. *J. Vertebr. Paleontol.* **37**, e1312690 (2017).
37. L. Cavin, P. L. Forey, S. Giersch, Osteology of *Eubiodectes libanicus* (Pictet & Humbert, 1866) and some other ichthyodectiformes (Teleostei): phylogenetic implications. *J. Syst. Palaeontol.* **11**, 115–177 (2013).
38. B. Schaeffer, C. Patterson, Jurassic fishes from the western United States, with comments on Jurassic fish distribution. *Am. Museum Novit.* **2796**, 1–86 (1984).
39. G. Arratia, New remarkable Late Jurassic teleosts from southern Germany: Ascaloboidae n. fam., its content, morphology, and phylogenetic relationships. *Foss. Rec.* **19**, 31–59 (2016).
40. M. Friedman, Parallel evolutionary trajectories underlie the origin of giant suspension-feeding whales and bony fishes. *Proc. R. Soc. B Biol. Sci.* **279**, 944–951 (2012).
41. M. Friedman, *et al.*, 100-million-year dynasty of giant planktivorous bony fishes in the Mesozoic seas. *Science (80-.).* **327**, 990–993 (2010).
42. A. Tintori, The actinopterygian fish *Prohalecites* from the Triassic of Northern Italy. *Palaeontology* **33**, 155–174 (1990).

43. L. Wretman, H. Blom, B. P. Kear, Resolution of the Early Jurassic actinopterygian fish *Pachycormus* and a dispersal hypothesis for Pachycormiformes. *J. Vertebr. Paleontol.*, e1206022 (2016).
44. P. M. Brito, Révision des Aspidorhynchidae (Pisces, Actinopterygii) du Mésozoïque : ostéologie, relations phylogénétiques, données environnementales et biogéographiques. *Geodiversitas* **19**, 681–772 (1997).
45. P. E. Olsen, A. R. McCune, Morphology of the *Semionotus elegans* species group from the Early Jurassic part of the Newark Supergroup of Eastern North America with comments on the family Semionotidae (Neopterygii). *J. Vertebr. Paleontol.* **11**, 269–292 (1991).
46. L. Grande, W. E. Bemis, A comprehensive phylogenetic study of amiid fishes (Amiidae) based on comparative skeletal anatomy. An empirical search for interconnected patterns of natural history. *J. Vertebr. Paleontol.* **18**, 1–696 (1998).
47. Z. Sun, *et al.*, A new non-parasemionotiform order of the Halecomorphi (Neopterygii, Actinopterygii) from the Middle Triassic of Tethys. *J. Syst. Palaeontol.* (2016) https:/doi.org/10.1080/14772019.2016.1181679.
48. A. E. Latimer, S. Giles, A giant dapediid from the Late Triassic of Switzerland and insights into neopterygian phylogeny. *R. Soc. Open Sci.* **5**, 180497 (2018).
49. D. Thies, J. Waschkewitz, Redescription of *Dapedium pholidotum* (Agassiz, 1832) (Actinopterygii, Neopterygii) from the Lower Jurassic Posidonia Shale, with comments on the phylogenetic position of *Dapedium* Leach, 1822. *J. Syst. Palaeontol.* **4**, 339–364 (2016).
50. M. Friedman, The early evolution of ray-finned fishes. *Palaeontology* **58**, 213–228 (2015).
51. G.-H. Xu, K.-Q. Gao, M. I. Coates, Taxonomic revision of *Plesiofuro mingshuica* from the Lower Triassic of northern Gansu, China, and the relationships of early neopterygian clades. *J. Vertebr. Paleontol.*, e1001515 (2015).
52. G.-H. Xu, X.-Y. Ma, A Middle Triassic stem-neopterygian fish from China sheds new light on the peltopleuriform phylogeny and internal fertilization. *Sci. Bull.* **61**, 1766–1774 (2016).
53. G.-H. Xu, L.-J. Zhao, K.-Q. Gao, F.-X. Wu, A new stem-neopterygian fish from the Middle Triassic of China shows the earliest over-water gliding strategy of the vertebrates. *Proc. R. Soc. B Biol. Sci.* (2012) https:/doi.org/10.1098/rspb.2012.2261.
54. F. J. Poyato-Ariza, S. Wenz, A new insight into pycnodontiform fishes. *Geodiversitas* **24**, 139–248 (2002).
55. S. Giles, G. H. Xu, T. J. Near, M. Friedman, Early members of “living fossil” lineage imply later origin of modern ray-finned fishes. *Nature* (2017) https:/doi.org/10.1038/nature23654.
56. C. Romano, W. Brinkmann, Reappraisal of the lower actinopterygian *Birgeria stensioei* Aldinger, 1931 (Osteichthyes; Birgeriidae) from the Middle Triassic of Monte San Giorgio (Switzerland) and Besano (Italy). *Neues Jahrb. für Geol. und Paläontologie, Abhandlungen* **252**, 17–31 (2009).
57. T. Argyriou, *et al.*, Internal cranial anatomy of Early Triassic species of †*Saurichthys* (Actinopterygii: †Saurichthyiformes): implications for the phylogenetic placement of †saurichthyiforms. *BMC Evol. Biol.* **18**, 161 (2018).
58. J. Lu, S. Giles, M. Friedman, J. L. den Blaauwen, M. Zhu, The oldest actinopterygian highlights the cryptic early history of the hyperdiverse ray-finned fishes. *Curr. Biol.* **26**, 1602–1608 (2016).
59. S. Giles, *et al.*, Endoskeletal structure in *Cheirolepis* (Osteichthyes, Actinopterygii), an early ray-finned fish. *Palaeontology* (2015) https:/doi.org/10.1111/pala.12182.
60. A. Tintori, *et al.*, Oldest stem Teleostei from the Late Ladinian (Middle Triassic) of Southern China. *Riv. Ital. Di Paleontol. E Stratigr.* **121**, 285–296 (2015).
61. A. Tintori, Fish taphonomy and Triassic anoxic basins from the Alps: a case history. *Riv. Ital. di Paleontol. e Stratigr.* **97**, 393–407 (1992).
62. D. Davesne, *et al.*, The phylogenetic origin and evolution of acellular bone in teleost fishes: insights into osteocyte function in bone metabolism. *Biol. Rev.* **94**, 1338–1363 (2019).
63. D. Davesne, F. J. Meunier, M. Friedman, R. B. J. Benson, O. Otero, Histology of the endothermic opah (*Lampris* sp.) suggests a new structure–function relationship in teleost

fish bone. *Biol. Lett.* **14**, 20180270 (2018).
64. R. Zambelli, Note sui Pholidophoriformes: VII contributo *Eopholidophorus forojuliensis* n.g., n.sp. *Gortania* **11**, 63–76 (1990).
65. A. Tintori, *et al.*, New specialized basal neopterygians (Actinopterygii) from Triassic of the Tethys Realm. *Geol. Insubrica* **10**, 13–20 (2008).
66. A. Tintori, C. Lombardo, D.-Y. Jiang, Z.-Y. Sun, "*Pholidophorus*" *faccii* Gortani 1907 : nuovi dati tassonomici. *Gortania* **32**, 45–52 (2010).
67. N. Wadeson, M. Basham, Savu: a Python-based, MPI framework for simultaneous processing of multiple, N-dimensional, large tomography datasets. *arXiv*, arXiv:1610.08015 (2016).
68. D. Paganin, S. C. Mayo, T. E. Gureyev, P. R. Miller, S. W. Wilkins, Simultaneous phase and amplitude extraction from a single defocused image of a homogeneous object. *J. Microsc.* **206**, 33–40 (2002).
69. D. Gürsoy, F. De Carlo, X. Xiao, C. Jacobsen, TomoPy: a framework for the analysis of synchrotron tomographic data. *J. Synchrotron Radiat.* **21**, 1188–1193 (2014).
70. S. Sanchez, P. E. Ahlberg, K. M. Trinajstic, A. Mirone, P. Tafforeau, Three-dimensional synchrotron virtual paleohistology: a new insight into the world of fossil bone microstructures. *Microsc. Microanal.* **18**, 1095–1105 (2012).
71. A. Mirone, E. Brun, E. Gouillart, P. Tafforeau, J. Kieffer, The PyHST2 hybrid distributed code for high speed tomographic reconstruction with iterative reconstruction and a priori knowledge capabilities. *Nucl. Instruments Methods Phys. Res. Sect. B* **324**, 41–48 (2014).
72. A. Lyckegaard, G. Johnson, P. Tafforeau, Correction of ring artifacts in X-ray tomographic images. *Int. J. Tomogr. Stat.* **18**, 1–9 (2011).